

Geometry and stability of species complexes: larger species speciate less often

Amaury Lambert, Emmanuel Schertzer, Yannic Wenzel

April 1, 2025

Abstract

Species complexes are groups of closely related populations exchanging genes through dispersal. We study the dynamics of the structure of species complexes in a class of metapopulation models where demes can exchange genetic material through migration and diverge through the accumulation of new mutations. Importantly, we model the ecological feedback of differentiation on gene flow by assuming that the success of migrations decreases with genetic distance, through a specific function h . We investigate the effects of metapopulation size on the coherence of species structures, depending on some mathematical characteristics of the feedback function h . Our results suggest that with larger metapopulation sizes, species form increasingly coherent, transitive, and uniform entities. We conclude that the initiation of speciation events in large species requires the existence of idiosyncratic geographic or selective restrictions on gene flow.

1 Introduction

The interplay of mechanisms underlying the emergence of biological diversity continues to captivate the scientific community engaged in evolutionary biology. The forces promoting or hindering the development of high species diversity are still largely unknown, as is the structure of the resulting reproductive networks ([1]). Phenomena such as ring species, which have provoked much thought within evolutionary biology (see [2]), show how diverse the structure of species complexes can be, raising the question: What general insights can be drawn about the structure of a species complex, and how does it influence the emergence of new species?

Speciation is the process by which diverging populations become reproductively isolated from each other, preventing them from producing offspring or ensuring that any offspring are inviable or sterile. The development of reproductive isolation (RI) relies on the accumulation of isolating barriers, i.e., the biological features that impede gene exchange between populations (see [3], p. 29). If this accumulation leads to substantial (but not

Glossary

Species complex: a set of populations connected through direct or indirect (i.e., through intermediary populations) gene exchange.

Feedback effect: the relationship between genetic distance and effective migration rates between populations whereby reduced effective migration rates reduce genetic similarity, further reducing gene flow, etc.

Genetic incompatibilities: post-zygotic reproductive barriers that lead to inviability, sterility or other genetic defects in hybrids.

Feedback function: a continuous function h , which encodes the reduction of effective migration rates due to genetic incompatibilities.

Transitivity: a property of species complexes ensuring that for any three populations i, j, k such that i can interbreed with j , and j can interbreed with k , then i can interbreed with k (e.g. ring species).

Clustering: species complex partitioned into clusters of highly genetically related populations but with lower genetic exchange between clusters (partial reproduction isolation).

Reversibility: a property of speciation that describes whether accumulated reproductive barriers between diverging populations can be reversed so that the reproductive isolation that has been built up disappears

necessarily complete) reproductive isolation, such as pre-mating isolation or hybrid sterility and/or inviability, we speak of different species (see [3], p.26ff). We emphasize that in fact, empirical data suggest that related species rarely exhibit complete reproductive isolation (see [3], p.33ff, [4]).

In general, we distinguish speciation processes by the extent to which geographic conditions impede gene flow. In perfect geographic segregation and zero gene flow (allopatry), the accumulation of different mutations leads to populations being reproductively isolated from each other at a secondary contact. Under geographic conditions allowing for limited gene flow, a combination of forces including natural and sexual selection can lead to the evolution of reproductive barriers between migrating populations (see [3], Sections 3 and 4).

Although it has been suggested that they may be quite common in nature (see [3], p.111ff, [5]), parapatric speci-

ation processes seem to have received relatively little attention in evolutionary modelling compared to allopatric or sympatric speciation (see [6], p.748). Recently, a new class of general speciation models started gaining popularity: a population- or individual-based framework, in which the degree of divergence between spatially dispersed groups of organisms is measured by their genetic distance (see [6], p.745ff for a review). Within this class of models, diversity between populations arises from mutations (increasing genetic distance), while homogeneity arises from migrations between populations (decreasing genetic distance). In fact, the increase in genetic distance following mutation events is based on the infinite-allele assumption that states that each mutation at a locus results in an allele of a novel type. On the other hand, genetic distance between populations tends to decrease following migration events, due to the fixation of part of the migrant genome in a resident population.

In most of these models (see for instance [7–9]), populations migrate between each other at a constant rate, independent of genetic distance (exceptions including [10], in the form of an individual-based assortative mating framework, and [11], for parapatric speciation between two populations). Once sufficient divergence took place, the classification as a new species is usually defined by the crossing of a predefined critical threshold of genetic distance between populations. By exceeding this threshold, the degree of reproductive isolation between the affected populations is typically assumed to jump from no isolation to complete isolation.

In this paper, we present a simple stochastic ‘genetic distance’ model in which the emergence of complete reproductive isolation occurs without jumps, as a natural consequence of the interaction between gene flow and genetic distance between populations exposed to migration. In fact, through the coupling of migration rates to genetic distance, speciation results from an initial increase in genetic distance causing migration rates to decrease, which tends to increase genetic distance further, and so on. One can think of this dynamic as a positive feedback loop, which causes divergent populations to naturally snowball into complete reproductive isolation. We establish a general framework for the study of species complexes that is suitable to describe the emergence and stability of complex interbreeding structures, such as ring species.

The integration of this feedback effect into the model through the function h , which encodes the translation of genetic distance to effective migration rates, raises some intriguing questions: Can we link characteristics of species complexes, such as transitivity, clustering, or stability, to analytical properties of the function h ? Between geographic migration restrictions and genetic incompatibilities that reduce gene flow, which force has a

stronger influence on the shape of large species complexes? And finally, can we infer information about quantities related to speciation, such as reversibility, the distribution of time to first speciation, or the average number of new species from the structure of a species complex?

2 Model description

In this Section, we present the idea of the model, the underlying biological assumptions and its mathematical implementation.

Evolutionary feedback.

The central idea of the model is to understand speciation as a consequence of a self-sustaining interaction between effective migration rates and the difference in genetic architecture between populations exposed to migration. Here, we use the term “effective migration rate” to refer to the rate at which an individual migrates from one population to another, and fixes part of its genetic material in the arrival population. As alluded to above, the coupling of effective migration rates to genetic proximity can cause speciation by an initial decrease in genetic proximity (due to mutation) causing effective migration rates to decrease, which tends to decrease genetic proximity further, and so on. We will refer to this dynamic as the **feedback effect**.

The term “difference in genetic architecture between populations” is intentionally kept broad, in order to encompass different modeling approaches to speciation. For instance, this difference could refer to different genetic configurations at neutral “speciation genes” between populations. In the spirit of [12], neutral in this context refers to the assumption that no selection is acting on the genes other than that resulting of hybrid depression. It is well known that typically not all genes are involved in the evolution of reproductive isolation. The number of these “speciation genes” (see [13] for a precise definition and review of this term) can be as little as two, or reach into the hundreds, depending on the populations one considers (see [3], p.302).

Another interpretation of the genetic difference between populations is the net synonymous divergence, i.e. the number of substitutions of one base pair for another in coding regions of the genome such that the amino acid sequence produced is not altered. Data from different animal populations/species (see [4] and, for instance, Fig. 3 therein) indicate that the net synonymous divergence between populations serves as a good proxy to measure the degree of reproductive isolation between populations. This fact makes this interpretation especially appealing from an application point of

view, because synonymous substitutions are much easier to quantitatively determine than speciation genes.

The analysis of data in [4] further shows that there is only a relatively narrow region in which determining the species boundaries is difficult, coined as the gray zone of speciation. In this region, a given degree of neutral divergence corresponds to different isolation levels between taxa. To encapsulate these different isolation regimes, we will consider a function that takes the genetic divergence between populations as an input, and returns the reduction in effective migration rate specific to a given pair of populations/species. We will denote this function by h , and refer to it as the **feedback function**.

We emphasize that estimates of these isolation regimes exist, and can serve as a good proxy for the shape of the feedback function h . As alluded to above, in [4] the authors estimate the probability of ongoing migration between two populations/species as a function of their genomic divergence at synonymous sites, from observed genomic data (see, for instance, [4] Fig. 3). The results indicate that across various animal species and populations, the probability of ongoing migration drops once divergence affects a critical number of sites. The feedback function h , specific to a population/species pair, can be thought of as encapsulating the shape and speed of this drop.

By coupling the effective migration rate to the genetic proximity of two populations, we can understand speciation as the diverse process it is understood to be. Speciation is neither always a sudden, nor always a gradual process. Examples from nature can be found at either end of the spectrum, see [3, 14]. However, most speciation models (see for instance [9, 15]) focusing on the genetic distance between populations rely on the crossing of a predefined threshold in order to achieve complete reproductive isolation. In this Heaviside step function framework, there is no feedback between differentiation and reproductive isolation: as long as genetic proximities are above the jumping-threshold, the effective migration rates stay constant. Once the genetic proximity between two populations falls below this level, reproductive isolation is complete and the frequency of migration events can go from high to zero in one fell swoop. As mentioned above, effective migration rates are known to exhibit different behaviors (see for example [4, 16]), which motivates the incorporation of a feedback function that allows expressing different strengths of reduction in effective migration rates associated to genetic divergence.

Effective migration and mutation.

In this paper we use the Biological Species Concept (BSC) as elaborated in [3], p.30: We refer to speciation as the process by which two biological populations

become reproductively isolated.

Most known reproductive barriers amount to genetic differences (see [3], p.36). There are exceptions, where reproductive isolation amounts to behavioral incompatibilities or ecological factors (for instance, the disappearance of an appropriate ecological niche), see [17]. Here, we will apply an adapted version of the BSC presented above, modeling only the reproductive barriers that are associated to genetic differences. Hence, we will measure the degree of reproductive isolation between two populations solely as a function of their genetic differences at neutral sites. Before we can define this function, we must first say what we mean by the genetic difference between two populations - because of genetic variation, we cannot assign a single genotype to an entire population without making additional assumptions.

We suppose that populations are distributed among N islands (or island-like areas), see [18] for a general framework of the meta-population modeling approach to speciation. Further, we consider the genetic architecture of the N populations at $L \in \mathbb{N}$ loci. Genetic diversity between populations emerges from the interplay of two forces: mutation and migration. Mutation events tend to increase genetic diversity, while migration events tend to homogenize the genetic material among populations.

As alluded to above, we assume the absence of intra-population polymorphism, i.e., of multiple different phenotypes within a population, for the genes under consideration. To ensure that this property holds after mutation or migration events, we assume that the time between the appearance and loss/fixation of an allele is significantly shorter than the waiting time between two events. Thus, one conventionally ignores the short phases during which the population is polymorphic due to multiple segregating mutant alleles at a given site (see [19, 20] for reviews).

In the same spirit as in Roux et al. [4], this means that we understand effective migration rates, defined as the rate at which an individual from one population migrates to another, and fixes "almost instantaneously" a fraction of its genetic material in the arrival population. Likewise, in the context of mutation events, we only consider effective mutation rates, where a new mutant appears and "instantaneously" achieves fixation.

In our model, we will further make the simplifying assumption that migration events always result in fixation at a single locus in the arriving population. In order to justify this assumption, we first note that if recombination rates are high enough, this will cause substantial fragmentation of the mutant genome and break genetic correlations. Then, after a few generations, the linkage disequilibrium becomes very small, and we can expect alleles to fix independently. Under a neutrality assumption for the L genes, the number of migrant

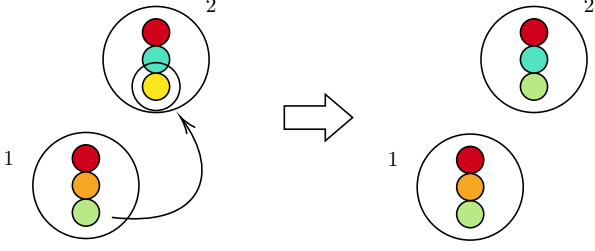


Figure 1: Toy realisation of the model and a migration event. Here, we have $N = 2$, $L = 3$, and the migration occurs from population 1 to 2, affecting locus 3. The genetic proximity between 1 and 2 changes from $1/3$ to $p_{12} = 2/3$.

alleles fixating in a population of size n is thus given by a Binomial random variable with parameters $(\frac{1}{n}, L)$. Hence, if $n \gg L$, then conditional on some fixation (i.e., at least one fixation of a mutant allele in the resident population), this fixation affects exactly one locus with high probability. Finally, we note that our assumption of fixation at a single locus is mainly made out of mathematical convenience and that our model could be easily adapted to multi-loci fixations but at the cost of analytical tractability.

As already mentioned, we only consider mutation events within subpopulations that lead to fixation. In the realm of neutral theory, the effective mutation rate per site μ can be directly identified with the individual mutation rate per site [21].

The model.

Now, consider $N \in \mathbb{N}$ populations of n_1, \dots, n_N sexually reproducing organisms, each population monomorphic for $L \in \mathbb{N}$ speciation loci. In the following, lower case letters represent the populations and upper case letters the loci. We will represent the state of the model by a matrix of types $A^L(t) := (A_{i,K}^L(t))_{i \in [N], K \in [L]}$ evolving in time, where $A_{i,K} := A_{i,K}^L$ represents the allelic type on island i at locus K . Note that $A_{i,K}$ depends implicitly on L , but we omit to indicate this dependence to ease the notation. The dynamics between the N island-populations will depend on a coupling factor between the loci. This coupling is enforced through the **genetic proximities**, defined between any population i and j by

$$P_{ij}^L(t) := \frac{1}{L} \sum_{K=1}^L \mathbf{1}_{\{A_{i,K}(t) = A_{j,K}(t)\}}. \quad (1)$$

Here, the notation $\mathbf{1}_{\{A_{i,K}(t) = A_{j,K}(t)\}}$ is defined through

$$\mathbf{1}_{\{A_{i,K}(t) = A_{j,K}(t)\}} = \begin{cases} 1 & \text{if } A_{i,K}(t) = A_{j,K}(t) \\ 0 & \text{otherwise} \end{cases}.$$

In words, the genetic proximity between i and j is the fraction of loci at which population i and j currently carry the same allele.

The model depends on the following parameters:

- the mutation rate $\mu > 0$,
- the migration matrix $(m_{ij})_{i \neq j}$, where $m_{ij} \geq 0$ are migration rates, reflecting potential geographic restrictions,
- and an increasing function h on $[0, 1]$, verifying $h(0) = 1 - h(1) = 0$, called the feedback function

The dynamics of the model are governed by two antagonistic forces: mutation and migration. In any population $i \in [N]$, at any locus $K \in [L]$, **mutation** events occur at rate μ . Any (i, K) experiencing a mutation event takes on a new type (∞ -allele model). For any time $t \geq 0$, between any populations i and j , and at any locus $K \in [L]$, **migration** events from i to j occur at rate

$$m_{ij} h(P_{ij}^L(t)). \quad (2)$$

In the type matrix, this amounts to replacing the type of j by the type of i at locus K , see Fig. 1.

We note that after a mutation event, the genetic proximity between the concerned population i (at some locus K) and every other population j decreases by $1/L$, if i did not already carry a different allele than j at locus K before. Furthermore, after a migration event from i to j (at some locus K), the genetic proximity between i and j is increased by $1/L$ if i and j carried different allelic types prior to the migration event.

3 ODE approximation and duality

In this Section, we describe how our stochastic model can be approximated by the solution to an ordinary differential equation (ODE), when the number of loci is sufficiently large. This result will allow us to study the evolution of the genetic proximities over time in a deterministic context, and thus analytically derive properties of speciation events in our model.

More specifically, we will illustrate that the genetic proximities $(P_{ij}^L(t))_{i,j \in [N]; t \geq 0}$ in our stochastic model can be approximated by a continuous, deterministic function $P(t) := (P_{ij}(t))_{i,j \in [N]}$, solution to the non-

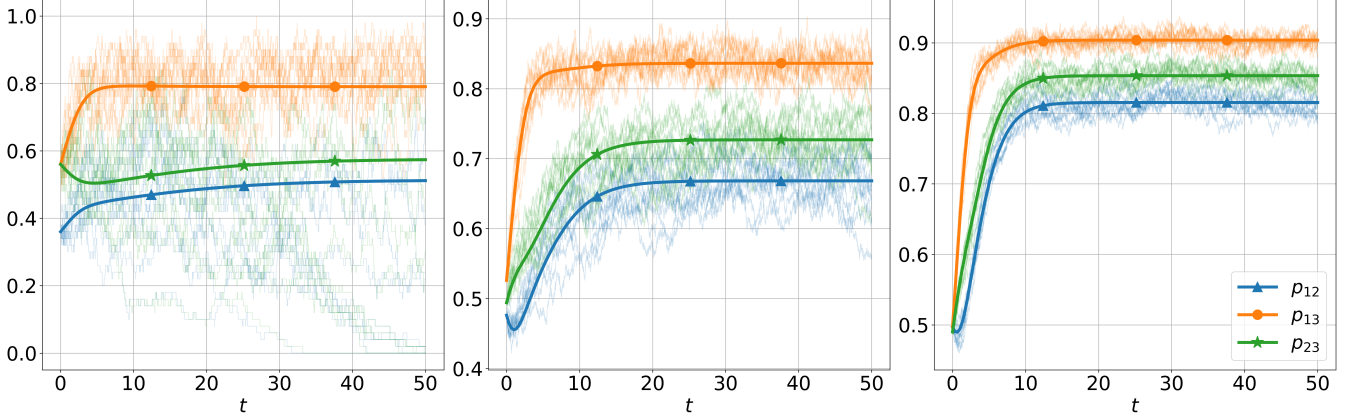


Figure 2: Convergence of the stochastic genetic proximities to the solution of the ODE for 3 populations. The strong, solid lines are numerically simulated solutions to the ODE (3). The transparent lines are simulations of the stochastic model for different numbers of loci, namely $L = 50, 500, 1000$ from left to right. Additionally, we varied mutation rates, namely $\mu = 0.1, 0.08, 0.05$ from left to right, while keeping the migration matrix constant: $M = ((0, 0.1, 0.8), (0.1, 0, 0.5), (0.8, 0.5, 0))$.

linear differential equation

$$\begin{aligned} \dot{P}_{ij} &= \sum_{k=1}^N (m_{ik}h(P_{ik})P_{kj} + m_{jk}h(P_{jk})P_{ik}) \\ &- P_{ij} \left(\sum_{k=1}^N (m_{ik}h(P_{ik}) + m_{jk}h(P_{jk})) + 2\mu \right), \end{aligned}$$

for all $i \neq j \in [N]$. This will be written shortly as

$$\dot{P}(t) = \vec{F}(P(t)). \quad (3)$$

Note that for $N = 2$ this ODE becomes

$$\dot{p} = 2mh(p)(1-p) - 2\mu p. \quad (4)$$

In Fig. 2, we illustrate the convergence of the stochastic genetic proximities to the solution of the ODE with simulations.

We now give a brief heuristics for the system of equations (3) and refer to the Appendix A for a rigorous derivation.

Consider the matrix of types

$$A := ((A_{i,K}(t))_{i \in [N], K \in [L]; t \geq 0})$$

we introduced in the previous Section. To gain some intuition, we start by assuming that $h \equiv 1$, so that the effective migration rates are not impacted by genetic distances (absence of feedback). In this setting, the allelic composition at each locus $K \in [L]$

$$A_K := ((A_{1,K}(t), \dots, A_{N,K}(t))(t) : t \geq 0)$$

evolves independently, according to a Moran model on a weighted graph. That is, each population is thought

of as an individual; new mutations arise at rate μ and "individual" j takes on the type of "individual" i at rate m_{ij} . In particular, when $m_{ij} = m$ for all $i \neq j$, this process corresponds to the standard Moran process, see [22].

How does changing h to a non-trivial feedback function influence the model? If h is not constant, the previous representation remains valid under an important adaptation: the reproduction rate m_{ij} in the case $h \equiv 1$ needs to be replaced by $m_{ij}h(P_{ij}^L)$. The resulting allelic processes A_1, \dots, A_L are now coupled through the genetic proximities P_{ij}^L , given by

$$P_{ij}^L(t) = \frac{1}{L} \sum_{K=1}^L \mathbf{1}_{\{A_{i,K}(t)=A_{j,K}(t)\}}. \quad (5)$$

For small values of L , this induces a strong interaction between loci. However, for a large number of loci, the interactions between any pair of loci should become negligible. Thus, under the premise that the loci are asymptotically uncorrelated, we can apply the law of large numbers to obtain the convergence of $P_{ij}^L(t)$ to a deterministic quantity. This limit, which we will denote by $P_{ij}^\infty(t)$, describes the coupling between the allelic processes (A_1, \dots, A_L) , when the number of loci is large. Furthermore, all the limiting allelic processes should be identically distributed, since the property holds true for finite L . Let $\mathcal{A} := (\mathcal{A}(t))_{t \geq 0}$ be the limiting allelic process. Intuitively, we think of \mathcal{A} as the allelic process at a "typical" locus.

Can we provide a description of the dynamics of the limiting allelic process \mathcal{A} ? To deduce the reproduction rates, we recall that for finite L , the rate at which j takes

on the type of i is

$$\begin{aligned} m_{ij}h(P_{ij}^L(t)) &= m_{ij}h\left(\frac{1}{L}\sum_{K=1}^L \mathbf{1}_{\{A_{i,K}(t)=A_{j,K}(t)\}}\right) \\ &\approx m_{ij}h(\mathbb{P}(\mathcal{A}_i(t) = \mathcal{A}_j(t))) \quad (\text{as } L \rightarrow \infty) \end{aligned}$$

where in the last line, we used the law of large numbers.

We obtain a single-locus Moran representation of our stochastic model via the process \mathcal{A} , whose dynamics are given as follows. At rate μ at every $i \in [N]$, mutations occur. Given a mutation event, an individual takes on a new type. At time $t \geq 0$ and at rate

$$m_{ij} \cdot h(\mathbb{P}(\mathcal{A}_i(t) = \mathcal{A}_j(t)))$$

reproduction events from i to j occur, that is, the individual j takes on the type of i .

The representation of P_{ij}^L in equation (5) gives an interpretation of the limiting P_{ij} in terms of the allelic process \mathcal{A} , i.e.,

$$P_{ij}^L(t) \rightarrow P_{ij}^\infty(t) := \mathbb{P}(\mathcal{A}_i(t) = \mathcal{A}_j(t)), \quad (6)$$

that is, $P_{ij}^\infty(t)$ is the probability that i and j have the same type at time t on the Moran model \mathcal{A} describing the dynamics at a "typical" locus. Since we will now only consider the limiting processes $(P_{ij}^\infty(t))$, we will define $P_{ij}(t) := P_{ij}^\infty(t)$ to ease the notation.

To understand the evolution of the limiting P_{ij} 's, it remains to capture the evolution of the allelic process \mathcal{A} . This process is an example of a *nonlinear* Markov process, characterized by the dependence of the transition probabilities not only on the state, but also on the process distribution (here the probability that two sites have the same allelic type). The term *nonlinear* represents the non-linearity in the Chapman-Kolmogorov equation, that the transition probabilities of the Markov process satisfy. We will call \mathcal{A} a *nonlinear* Moran process.

Crucially, the nonlinear Moran process \mathcal{A} allows us to express the deterministic genetic proximities P_{ij} as the solution to a system of ODEs. This property can be seen by the "backward" representation of the Moran process thanks to a duality approach.

To gain some intuition, consider the process \mathcal{A} at equilibrium, i.e., when the quantities $P_{ij}(t)$ have attained their equilibrium state P_{ij}^{eq} . In this case, the process \mathcal{A} corresponds to a Moran process on a weighted graph. We consider its graphical representation on $[N] \times \mathbb{R}_+$ (see [22]):

- For a reproductive event $i \rightarrow j$ at time t , draw an arrow with origin at (i, t) and tip at (j, t)
- For a mutation event at site k at time t , draw a \star at (k, t) .

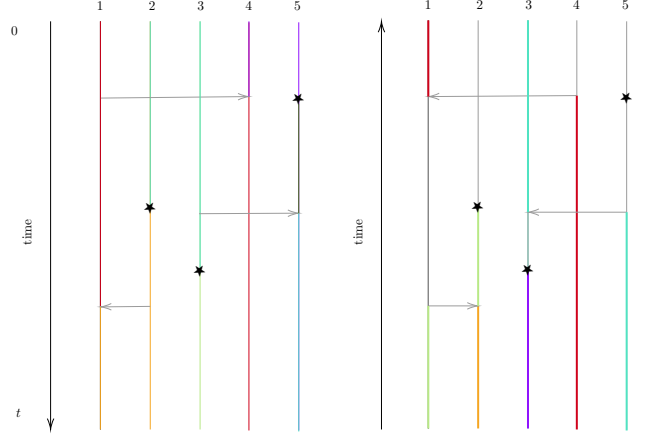


Figure 3: Realisation of the genetic partitions induced by the single-locus Moran model, and its dual for $N = 5$. On the left, colours represent genetic types, whereas on the right, colours represent ancestral lineages.

Let us now consider the population at a reference time T . Via this graphical representation (see Fig. 3), we can associate to every individual an ancestral lineage using the arrow-star configuration. Then, the system of ancestral lineages is distributed like random walks on a graph: they evolve independently until they coalesce, jumping from site i to j at rate $m_{ij} \cdot h(P_{ij}^{\text{eq}})$. Each lineage is killed upon encountering a mutation (\star). This is because once an ancestral lineage encounters a mutation, no more information about the type of the lineage can be inferred, as the previous type is lost by the occurrence of the mutation.

By (6), the quantity P_{ij}^{eq} can be computed as the probability that i and j are of the same type. This occurs if and only if the ancestral lineages starting from i and j coalesce before being killed. Since the transition rates themselves depend on the genetic proximities, we obtain that P_{ij}^{eq} can be computed by solving a fixed point problem. More formally, define the coalescing time

$$T_{ij} := \inf\{u > 0 : S^i(u) = S^j(u)\},$$

where S^i, S^j are the ancestral lineages starting from site (i, T) and (j, T) . We note that the law of T_{ij} depends on $P^{\text{eq}} = (P_{ij}^{\text{eq}})_{i,j \in [N]}$ through the jump rates of the ancestral lineages, we will thus write $T_{ij} = T_{ij}(P^{\text{eq}})$. According to the previous argument, the matrix of genetic proximities P^{eq} satisfies the **fixed point problem**

$$\forall i \neq j \in [N], \quad P_{ij}^{\text{eq}} = \mathbb{E} \left(e^{-2\mu T_{ij}(P^{\text{eq}})} \right). \quad (7)$$

If the $P_{ij}(t)$ now depend on time, the same argument applies, with the difference that the jump rates of the random walks become inhomogeneous in time. Using the same genealogical approach, we can compute the

probability that two sites i and j have the same type at some instant $t \geq 0$ by tracing their ancestral lineages back in time, starting from t . This allows us to deduce that $P_{ij}(t)$ are solution to the differential equation (3). We refer to Proposition B.1 and Corollary B.2 for details.

4 A special case: two populations

To get some intuition about how the fixed-point equation (7) relates to the ODE (3) we first consider the simplest possible case $N = 2$, with symmetric migration $m = m_{12} = m_{21}$.

Denote the one-dimensional, associated equilibrium P_{12}^{eq} by p^{eq} . In this case, the distribution of the random variable T_{12} is given by the minimum of two exponential random variables with parameter $mh(p^{\text{eq}})$ since coalescence occurs at the first jump of one of the two random walks. This minimum is an exponential law of parameter $2 \cdot mh(p^{\text{eq}})$ and the fixed point equation (7) writes

$$p^{\text{eq}} = \frac{mh(p^{\text{eq}})}{\mu + mh(p^{\text{eq}})} =: f(p^{\text{eq}}). \quad (8)$$

which coincides with the equilibrium condition for the ODE (4).

Let us now turn to the stability analysis of the ODE. We remark that $p^{\text{eq}} = 0$, corresponding to speciation between populations 1 and 2, is always an equilibrium. According to (4), 0 is a stable equilibrium if and only if

$$\left. \frac{df}{dp} \right|_{p=0} = \frac{mh'(0)}{\mu} < 1. \quad (9)$$

In words, if migration between the two populations ceases for a limited time, leading to some evolutionary divergence, they might resume gene flow upon a secondary contact if (9) is not verified.

If $h'(0) > 0$ implies that reproductively isolated populations could fuse upon a secondary contact, if migration rates are sufficiently large. The occurrence of such fusions would be problematic and contradict the general belief that complete reproductive isolation is irreversible (see [3], p. 37f, and [23]). Therefore, we must and will suppose throughout the rest of the article

$$h'(0) = 0. \quad (10)$$

We also show in the appendix that in higher dimension ($N > 2$), this condition guarantees that if several species complexes are in reproductive isolation, the configuration is also stable upon secondary contact. See Proposition C.6 in the Appendix for a precise statement and a proof.

Before closing this Section, let us emphasize that if the ODE approach seems much more direct in the case $N = 2$, it is far from obvious how to assess its general behavior in large species complexes. This already hints at an observation we will address in later sections: the two approaches presented are complementary in the sense that the ODE approach is well suited to describe small meta-populations, while the fixed-point problem is well suited to describe large meta-populations.

5 Intransitive species

Phenomena such as ring species or hybrid zones show how diverse the shapes of species complexes can be (see [2, 24]), begging the question: How does the feedback function determine the shape of a species complex?

We begin by defining the notion of species complexes in our framework. Let $P^{\text{eq}} = (P_{ij}^{\text{eq}})_{i,j \in [N]}$ be an equilibrium for the system of genetic proximities (27). We say that a group of populations $S \subseteq [N]$ forms a **species** if any two populations i and j therein can exchange genes: either directly (i.e., $h(P_{ij}^{\text{eq}}) > 0$), or through a chain of intermediary populations (i.e., there is $i = k_0, k_1, \dots, k_n = j \in [N]$ such that $h(P_{k_{l-1}k_l}^{\text{eq}}) > 0$ for all $l \in [n]$).

We first note that if i and j belong to the same species, then $P_{ij}^{\text{eq}} > 0$, reflecting the intuition that there is always some gene flow (either direct or indirect) within a species. Mathematically, this can be seen from the right hand side of the fixed point problem (7). Indeed, if i, j belong to the same species, then T_{ij} is almost surely finite and $\mathbb{E}[e^{-2\mu T_{ij}(P^{\text{eq}})}] > 0$. See also Proposition C.3 in the Appendix for a formal proof.

If we assume that $h > 0$ on $(0, 1]$, this property entails that individuals within the same species will always be able to interbreed. The situation is more complex if we assume that populations can not interbreed below a genetic threshold c , that is, when there exists c such that $h(x) = 0$ for $x < c$. In this case, we observe the emergence of intransitive hybridization networks, in the sense that if i can hybridize with j , and j can hybridize with k , i can not always hybridize with k . We provide two examples.

Friendship graph. First, we consider a complete migration graph with constant $m_{ij} = m$ of size $2K + 1$. By performing simulations (see 13), we demonstrate that we can choose a feedback function h , such that the species graph of Figure 4b is stable so that individuals can only interbreed if they belong to the same triangle. This example illustrates that despite the homogeneity of the underlying migration structure, non-transitive hybridization structures can emerge. Our simulations also reveal that the friendship graph can only exist at small enough

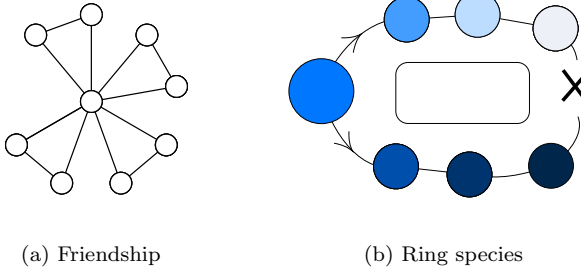


Figure 4: Species graphs corresponding to intransitive equilibria. On the left, friendship graph for $K = 4$, on the right, ring species with 7 populations. The terminal forms of the ring species population complex are reproductively isolated, despite ongoing gene flow through the chain of intermediary populations.

K , see Fig. 13. In the Appendix (see Proposition C.10), we demonstrate this property analytically.

Ring species. We now consider N populations in a ring migration structure, see Fig. 4b, with reduced migration between the two terminal populations. For the sake of illustration, we will assume that the effective migration rates are constant equal to m except at the end point where $m_{1,N} = m_{N,1} = \frac{m}{2}$. The geographic barrier that the ring evolves around corresponds to an area of unsuitable habitat, see for instance [25] for a valley separating salamanders or [26] a ring species in plants distributed across several islands.

In Fig. 5, we investigate the existence of a ring species where the two end populations 1 and N are reproductively isolated from each other, despite ongoing gene flow through intermediary populations. The simulations reveal that while requiring very specific conditions (small migration, low enough threshold), ring species can exist stably in a static environment.

6 Clustering within species

Partial reproductive isolation refers to a situation where two populations retain some ability to interbreed but face reproductive barriers that limit gene flow between them. Within our framework, this translates into the existence of species complexes partitioned into clusters of highly genetically related populations but with lower genetic exchange between clusters.

To illustrate this phenomenon, we consider the simplest migration setting with complete migration ($m_{ij} = m$ for every i, j). By considering (3), we first see that any symmetric vector P^{eq} , i.e., such that for all $i \neq j$,

$$P_{ij}^{\text{eq}} = p, \quad (11)$$

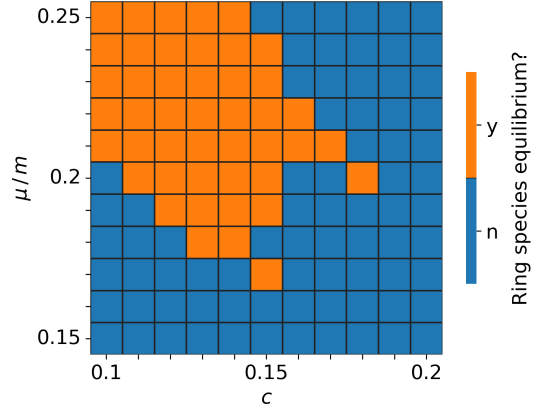


Figure 5: Existence of stable ring species equilibria in dependence of the mutation / migration ratio and the threshold value. We performed a systematic root search (as described in Fig. 8), but for ring species equilibria. Here, we set $h(x) = \mathbf{1}_{\{x \geq c\}} \frac{x-c}{1-c}$, $N = 6$.

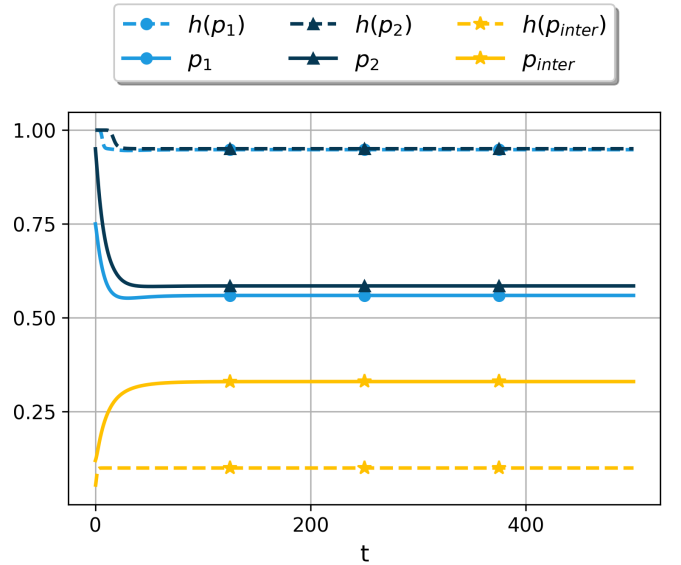


Figure 6: Clustering equilibrium in the symmetric case (for all $i \neq j, m_{ij} = m$). The plot displays genetic proximities over time. Here, we considered the feedback function h_2 , displayed on the right of Fig. 8. Further, we considered $\mu = 0.01, m = 0.02, |V_1| = 4, |V_2| = 6$.

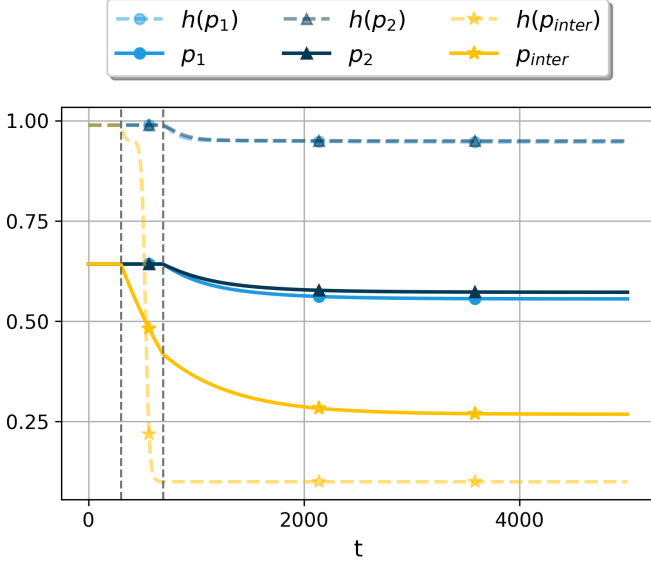


Figure 7: Multi-stability: Transition from symmetric to clustering equilibrium. In the time interval between the dotted vertical lines, migration rates between the nodes of V_1 and V_2 are set to zero. The plot displays genetic proximities over time. Here, we considered the feedback function h_2 , displayed on the right of Fig. 8. Further, we considered $\mu = 0.0055$, $m = 0.01$, $|V_1| = 3$, $|V_2| = 4$.

is a stable equilibrium if and only if the two following conditions are satisfied:

$$h(p)(1-p) = \frac{\mu}{m}p, \quad (12)$$

giving the equilibrium property, and

$$h'(p)(1-p) - h(p) - \frac{\mu}{m} < 0, \quad (13)$$

giving local stability. We remark that equation (12) is equivalent to the fixed point problem (8) in dimension 2, and in particular, independent of N . A natural question is whether there exist transitive equilibria that do not satisfy the symmetry property (11), that is, species complexes with groups of populations exhibiting higher genetic relatedness within patches than between them (partial reproductive isolation).

In Fig. 6 we consider the feedback h_2 as in Fig. 8. Intuitively, this function can be thought of as representing incompatibilities that arise in stages, with each plateau being interpreted as a degree of genetic incompatibility.

We now consider a case where $[N]$ is split into two sets of vertices V_1 and V_2 . We then consider equilibria P^{eq} with three degrees of freedom, namely, the genetic proximity within V_1 (denoted by p_1), the genetic proximity within V_2 (denoted by p_2), and the genetic proximity between V_1 and V_2 (denoted by p_{inter}). We observe the existence of stable equilibria with $p_1, p_2 > p_{\text{inter}}$,

thus showing that partially isolated clusters can coexist within the same species. An analytical treatment of this phenomenon is given in the Appendix, see Proposition C.9.

In Fig 7, we show how partial reproductive isolation can emerge from temporary geographic isolation. Namely, consider the splitting of $[N]$ into V_1 and V_2 from above, and genetic proximities at a symmetric equilibrium at time $t = 0$. At time $T > 0$, we impose isolation in a time window of duration t_{stress} so that we set $m_{ij} = 0$ if i and j belong to different V_k , for $k = 1, 2$. At time $T + t_{\text{stress}}$, we reestablish complete migration (i.e., $m_{ij} = m$). When carefully choosing the size of the isolation window given by t_{stress} , the genetic proximities converge to an asymmetric equilibrium. In fact, it suffices to choose the time window of isolation such that the genetic proximity between V_1 and V_2 falls into the basin of attraction of the smaller equilibrium, but not into the basin of the speciation equilibrium. Notice that the genetic proximity inside each group of vertices remains unchanged during the isolation window, because symmetric equilibria are independent of the number of populations, see equation (12).

7 Large meta-populations

The previous two sections have demonstrated that species can exhibit complex structures. First, we showed that when a speciation threshold is present, species graphs can be intransitive. But why are such features so rare in nature? We will argue that this rarity can be explained by the effects of large population sizes.

Secondly, we identified scenarios in which populations consistently interbreed while forming clusters that remain in partial isolation. While such configurations can persist in small meta-populations, we will argue that large species networks tend to become increasingly coherent, transitive, and uniform.

We begin by considering the case of symmetric migration. Previously, we showed that a suitable choice of the feedback function enable the existence of exotic equilibria such as intransitive inbreeding structures (friendship graphs) or species with clusters in partial reproduction isolation (clustering). However, in the Appendix, we show that those specific inhomogeneous equilibria can only exist for small values of N . This suggests that such exotic features can only persist in small species complexes.

In Fig. 8, we perform a systematic search of inhomogeneous equilibria when migration is symmetric. As conjectured, we observe the existence of a critical size N_c , such that for $N > N_c$, the ODE system (3) only exhibits symmetric stable equilibria. Thus, our numerical

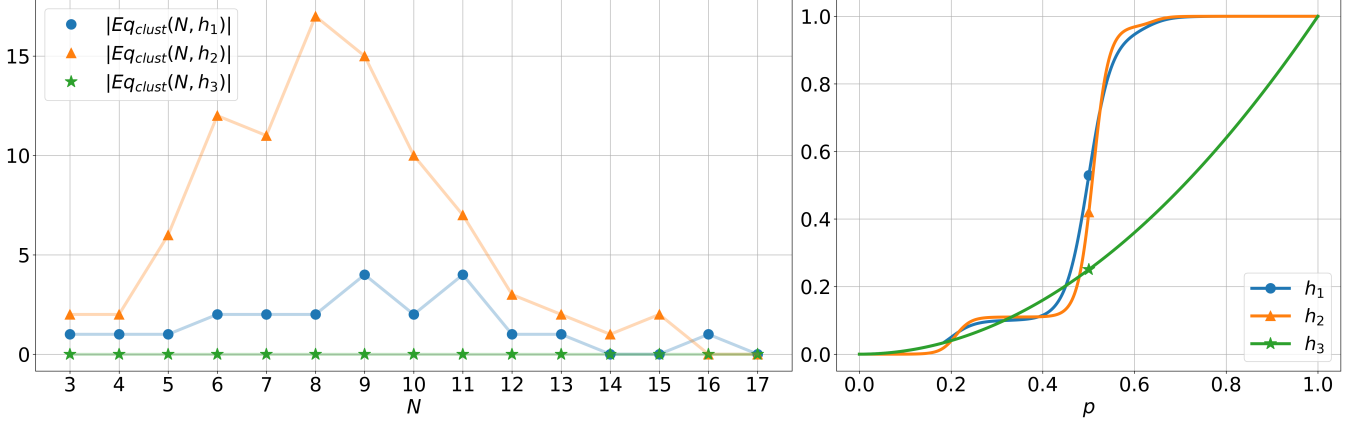


Figure 8: Disappearing of inhomogeneous equilibria, when N becomes large. On the left, we performed a systematic search for inhomogeneous roots of the function \vec{F} from (3), using a L-BFGS-B optimization algorithm. Then, we tested the roots stability by simulating the ODE (3), using the potential asymmetric root as initial position. The number of roots displayed corresponds to the number of different stable species graphs that were found. If two equilibria correspond to the same species graph (up to a permutation of nodes), they are not counted twice. On the right, we plotted different feedback functions, given by two smoothed versions of a step-function with jumps at $(s_1, s_2, s_3) = (0.12, 0.5, 0.63)$ to the steps $(y_1, y_2, y_3) = (0.1, 0.85, 1)$, and $h_3(x) = x^2$. The functions h_1 and h_2 differ mainly in their behaviour between 0 and s_1 , with h_1 not having a threshold and decaying like x^2 , and h_2 having a threshold. Further, we chose $\mu = 0.1$, $m = 0.42$.

simulations indicate that under symmetric migration, equilibria can only be symmetric for large enough meta-populations and the clustering effect previously observed can only hold for small populations (and presumably for a suitable choice of h).

In fact, we believe that the absence of clustering is valid not only for symmetric migration, but also for a much broader class of migration rates $(m_{i,j})$. To test this hypothesis, we consider populations of size N , where the migration rates m_{ij} , are independent and identically distributed. For the sake of illustration, we assumed a U -shaped distribution $\beta(.5, .5)$ so that the mass of this distribution is centered around the values 0 and 1, generating a strongly heterogeneous migration structure. In Fig. 9, we observe that as N gets large, the system equilibrates at a quasi-symmetric state.

Biologically speaking, this result suggests that most large species complexes should form rather simple and coherent structures. In particular, it follows that the specific migration rate between populations i and j does not have a strong influence on their genetic incompatibility. Intuitively, this can be understood from the fact that the main contribution of gene flow between i and j occurs through long and indirect paths. In fact, even if a significant geographical constraint substantially impedes direct gene exchange between the two populations, a large network guarantees that enough indirect migration paths (i.e., genes exchanges through many intermediary populations) between i and j outweigh this constraint. In this view, the gene flow between i and j should only

”feel” the average migration rate

$$m = \mathbb{E}(X) \quad (14)$$

This heuristics is confirmed by Fig. 9, where the quasi-symmetric equilibrium in a population with heterogeneous migration rate is well approximated by the symmetric equilibrium of a symmetric migration model with rates (14).

How can we understand this homogenization effect in general species complexes (and not only random)? We will now argue that if we make the further assumption that $m_{i,j}h(P_{ij}^{eq,N})$ ’s is uniformly bounded from below, then the equilibrium can only be symmetric despite the potential asymmetry of the migration network. In other words, if we restrict ourselves to the class of equilibria with a condition of minimal effective migration rates between any pair of populations, then the equilibria must be symmetric.

Heuristically, this surprising result is due to the fixed point property (7), and to the fact that random walks on a large, well connected graph reach their invariant distribution very quickly. More precisely, consider a large graph with $m_{i,j}h(P_{ij}^{eq,N}) > c$ for some constant c . Then, the large species graph $\left([N], (m_{i,j}h(P_{ij}^{eq,N}))_{i,j \in [N]}\right)_{N \in \mathbb{N}}$ is very well-connected, and does not exhibit bottlenecks (in fact, it is a family of expander graphs, see [27], p.38ff). Random walks on expander graphs attain their invariant distribution much faster than the time it takes two random walks to coalesce (see [28] or [29], p.4 for

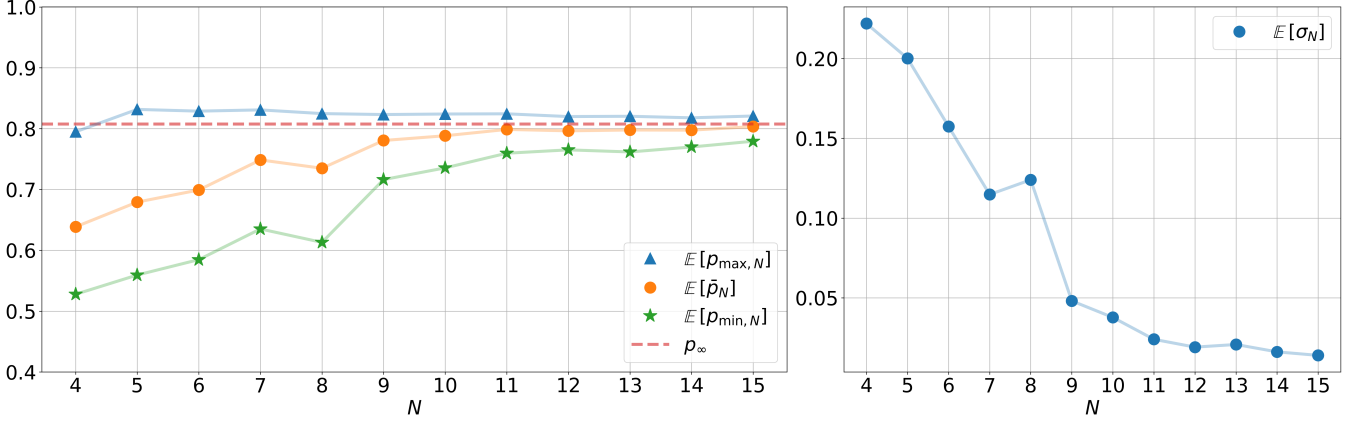


Figure 9: Convergence to symmetric equilibrium. On the left, we plotted means of different measures of the genetic proximities over 50 runs. Migration rates and initial conditions to the ODE (3) were taken *iid* according to a $\beta(0.5,0.5)$ distribution. Here, $p_{\max,N}$ respectively $p_{\min,N}$ corresponds to the minimum respectively maximum of the genetic proximities at equilibrium $((P_{ij}^{\text{eq}}))_{i,j \in [N]}$. Further, \bar{p}_N corresponds to the mean respectively the empirical standard deviation of the genetic proximities. Finally, p_∞ is the genetic proximity of the symmetric equilibrium associated to (14). On the right, we plotted the mean of the empirical standard deviation (normalised by the corresponding \bar{p}_N). The feedback function h was chosen as the function h_1 in Fig. (8). Additionally, we chose $\mu = 0.1$, and $m = 0.42$ for the mean migration rate.

coalescing times, and [27], p.40). Since the invariant distribution is independent of the starting position, this suggests that by the time the two random walks coalesce, they have forgotten their initial position. Thus, the fixed point property (7) would yield that $P_{ij}^{\text{eq},N}$ is the same for any i, j , and therefore symmetric. Furthermore, as we have seen in (14), the effect of homogenization is twofold in random networks. Not only are complex species symmetric at equilibrium, but an extra averaging effect on the $m_{i,j}$'s allows to deduce the genetic distances from the fixed point equation

$$h(p)(1-p) = \frac{\mu}{\mathbb{E}(m)}p.$$

8 Fluctuating migration networks

What are the implications of increased transitivity and coherence in large species complexes on their sensitivity to perturbation? To investigate this question, we consider a version of our model in which migration rates can change over time. For every edge, we re-sample the migration rates at rate $\theta > 0$.

We first consider that the migration rates are sampled according to a $\beta(.5, .5)$ distribution. We consider the first time to speciation τ , that is the random time at which the species complex breaks into two genetically isolated entities.

The results displayed in Fig. 10 indicate that the time to speciation increases sharply with the number of popu-

lations. Intuitively, this effect can be understood by the homogenization effect that we discovered for large static networks. Indeed, large species tend to form coherent and homogeneous structures and if resampling only impedes the migration rate between two populations, the loss in direct gene exchange is compensated by indirect migration paths (i.e., genes exchanges through many intermediary populations). Thus, we expect speciation to predominately occur when a single vertex i gets isolated by chance from the rest of the complex, that is, when all the migration rates $m_{i,j}$ are small. For large populations, this requires the coordination of many independent events so that speciation time should sharply increase with N as indicated by Fig. 10. Additionally, our initial intuition is confirmed from additional simulations (Fig. 12 in the Appendix) where we observed that speciation events typically involved a single population detaching from the species complex and forming its own species. This indicates that upon speciation, we can identify a mother species (the large component) and a daughter species (the small component). In particular, for large meta-population sizes, the predominant form of speciation will resemble peripatric speciation, with the difference that the large and small population complexes will continue to exchange some genes during divergence.

Additionally, Fig 10 reveals the sensitivity of speciation probabilities with respect to the feedback regime considered. In fact, although the maximal distance in the L^∞ -norm between the feedback functions h_i is significantly smaller than 0.1, the associated speciation probabilities can differ by values of up to 0.6. This indicates

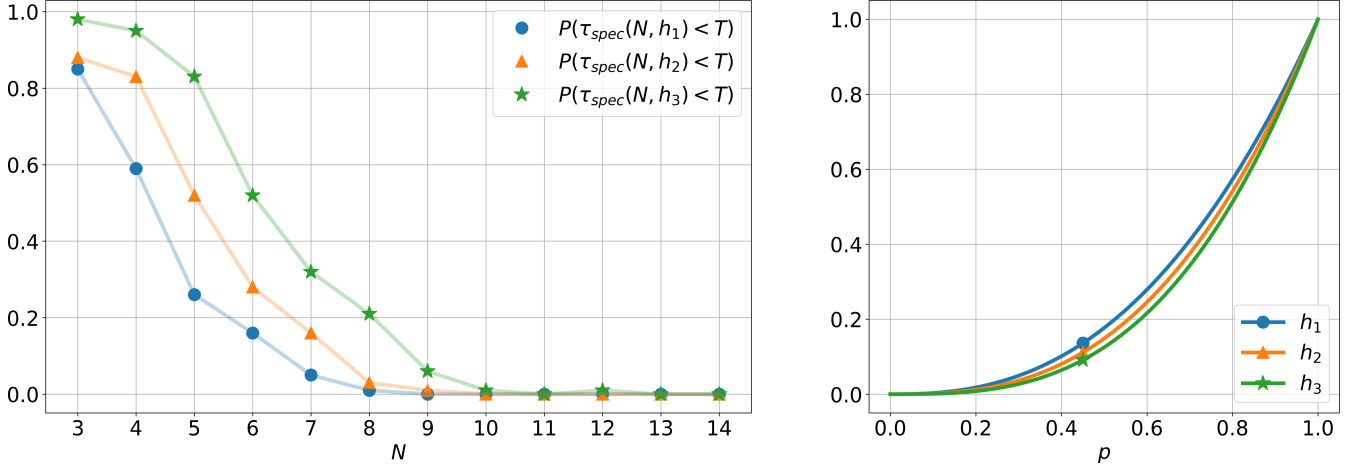


Figure 10: Decrease of speciation probability for different feedback regimes. We considered dynamically changing migration rates updated according to exponential clocks and resampled *iid* according to a rescaled Beta distribution. We plotted an estimation of the probability of speciation before a given time (here, $T = 200$) for different feedback functions, which are plotted on the right. Here, $h_1(x) = x^{2.5}$, $h_2(x) = x^{2.75}$, $h_3(x) = x^3$. Further, we chose $\mu = 0.1$, $m = \mathbb{E}[X] = 0.8375$, $\theta = 1$.

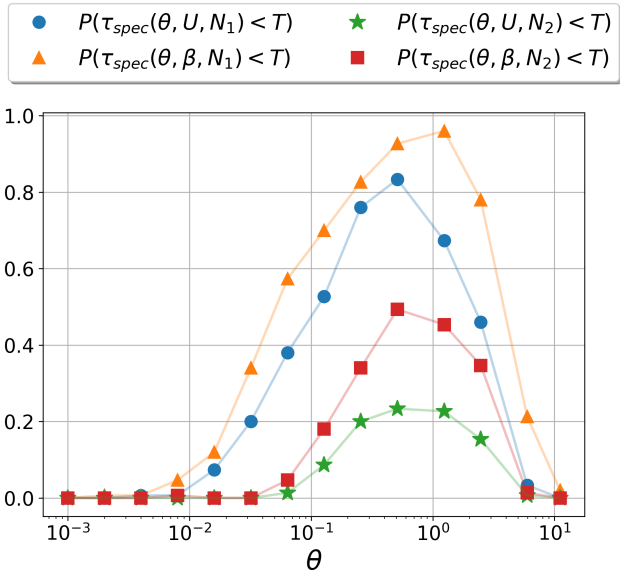


Figure 11: Speciation probability for different migration update distributions and values of N as a function of the rate of change of migration rate θ , estimated over 150 runs. The values $\tau_{\text{spec}}(\theta, U, N_i)$ resp. $\tau_{\text{spec}}(\theta, \beta, N_i)$ refer to the time of speciation with an migration update distribution given by $m_{\text{rate}} \cdot \mathcal{U}([0, 1])$ resp. $m_{\text{rate}} \cdot \beta(0.5, 0.5)$, and a number of populations given by $N = N_i$. Here, we chose $N_1 = 4$, $N_2 = 6$, $h(x) = x^3$, $\mu = 0.1$ and $m_{\text{rate}} = 1.675$.

a strong sensitivity of the time to speciation to the feedback function.

We investigate further the behavior of the speciation time in terms of the migration sampling rate θ , and different migration updating distributions. The simulations displayed in Fig. 11 suggest that for different sets of parameters, there exists a value $\theta_{\min}(N, m) > 0$, such that the speciation probability is at its maximum. At first glance surprisingly, the speciation probability decreases sharply when the rate of change of the environment is too large, i.e., when migration rates are updated too frequently. This can be explained heuristically by noting that in order to trigger a speciation event, geographic restrictions must be upheld for some time, allowing the positive feedback loop between genetic distance and effective migration rate to kick in. If migration rates are updated too quickly, the geographical constraints required for speciation will disappear too quickly for substantial divergence to occur.

Further, Fig. 11 shows that for small N , the speciation time depends heavily on the update distribution. Choosing a $\beta(0.5, 0.5)$ distribution as the update law, results in higher speciation probabilities than choosing a uniform distribution. This can be explained from the fact that a $\beta(0.5, 0.5)$ is a U-shaped distribution that produces values close to 0 with higher probability, and thus favors the occurrence of small migration rates which are needed to trigger speciation events.

This dependence on the migration update distribution is of particular interest in light of the fact that for large meta-population sizes, the populations should only “feel” the expected migration rate, which equals $1/2$ for both distributions.

9 Discussion

What are the causes of varying speciation rates across the tree of life? Numerous studies have explored the factors that may explain this diversity, including differences in geographic region, dispersal range, and selection (see [30–34]). This paper addresses the question by examining the structure of species complexes. Specifically, we investigate the effects of population sizes and the feedback strength between genetic distance and gene flow reduction on the transitivity and coherence of species structures. Our results suggest that with larger meta-population sizes, species form increasingly coherent, transitive, and uniform entities. Consequently, greater geographic constraints on gene flow are required to initiate speciation events, leading to a lower rate of speciation within larger meta-populations.

The model and an ODE approximation.

We started our investigation by presenting a neutral genetic distance model to study the evolution of genetic differences between N populations at L speciation loci. This stochastic model is parameterised by three parameters: the mutation rate μ , the migration matrix $(m_{ij})_{i,j \neq N}$, and a function h . The rate of effective migration events between two populations depends on potential geographical restrictions (through a migration matrix m_{ij}) and their genetic proximity (through the function h). Referred to as the feedback function, $h(p)$ encodes the extent to which a given degree of divergence (represented by the genetic proximity p) between two populations i and j reduces the effective migration rates between them.

The stochastic model can be well approximated by the solution to a non-linear ordinary differential equation (ODE), when the number of loci is large. This enabled us to analytically study the stability of reproductive structures at equilibrium within an ODE framework. Our first observation was that irreversibility of speciation requires the condition $h'(0) = 0$. In fact, if this condition is not verified, two reproductively isolated populations could resume gene flow and fuse again, given sufficiently strong migration rates m_{ij} . Such fusions would violate the irreversibility property of complete reproductive isolation (see [3, 23]).

Thus, speciation in our model arises when genetic distance and effective migration rates become trapped in a positive feedback loop, causing diverging populations to snowball into complete reproductive isolation. In fact, under the right conditions on μ and M , there may exist a stable migration-mutation equilibrium such that some populations are not reproductively isolated. However, in the case of $h'(0) = 0$, there is inevitably an unstable equilibrium below which we are trapped, since specia-

tion is always stable due to the irreversibility condition. Thus, once genetic proximities fall below the unstable equilibrium, they will always converge to the stable equilibrium of speciation.

The issue of transitivity in species complexes.

If we define a species complex as a set of populations connected through direct or indirect (i.e., through intermediary populations) gene exchange, what can we say about its structure? In particular, under which conditions can we expect the occurrence of intransitive species complexes like ring species? To this end, we consider two classes of feedback functions: with and without a threshold, i.e., a value $c \in [0, 1)$ such that two populations are completely reproductively isolated ($h = 0$) if their genetic proximity is smaller than c . In the absence of a threshold ($c = 0$), we showed that any two populations in the same species complex are able to exchange genes directly. However, when $c \in (0, 1)$, intransitive equilibria like ring species can occur, i.e., equilibria such that populations connected through indirect gene flow can be reproductively isolated. Strikingly, intransitive equilibria even exist in complete and symmetric migration, i.e. $m_{ij} = m > 0$ for all $i \neq j$, and we gave an example introduced as the friendship graph. Thus, transitivity of a species can be directly related to the behaviour of the feedback function around zero.

Clustering in species complexes.

In the presence of hybridisation between closely related species as in the case of grizzly-polar bear hybrids (see [35] or [36] for a general study), a non-trivial question relates to distinguishing whether occasional interbreeding between populations represents a transitory state on the way to speciation, or a stable equilibrium. Specifically, if a species is composed of population clusters of increased genetic relatedness that still exchange genes at low rates, do we observe speciation in progress, and can such genetic inhomogeneities within a species persist on an evolutionary time scale?

For small values of N , we showed that there exist species complexes with clusters of closely related sub-populations, that show little relatedness between clusters - even in the symmetric migration case. Furthermore, we observed that clustering within a species complex can emerge from a coherent unit by temporary isolation (multi-stability).

We emphasize that we showed existence of both intransitivity and clustering equilibria when the number of populations N is small. As it turns out, the transitivity and clustering properties of species complexes change completely when we consider large values of N .

Large meta-populations.

Our results suggest that clustering and intransitivity of species complexes in symmetric migration disappear when the number of populations is large. Surprisingly, this property of increased homogeneity and transitivity of species complexes seems to extend to any well-connected migration structure. In fact, when the number of populations is large, species complexes form transitive and relatively homogeneous entities where despite geographical heterogeneity, the genetic proximities between sub-populations remain homogeneous along the complex. This seemingly counter-intuitive behaviour can be explained by the observation that the degree to which any specific migration rate influences the shape of the entire species complex decreases, when the number of sub-populations increases. Indeed, in a well-connected large species complex, there are many paths connecting any two populations, and most of the gene flow occurs via long intermediary paths. As a consequence, the genetic proximity is not very sensitive to the direct migration rate between two populations and only the mean migration rate and the feedback function appear to determine the structure of the species complex at equilibrium.

Dynamics.

What are the implications of increased transitivity and homogeneity in a large species complex on its sensitivity to perturbation? As we alluded to above, reducing a specific migration rate between two populations has little influence on the structure of the species complex. This suggests that speciation rates should decrease for larger numbers of sub-populations.

We investigated our predictions on a dynamical migration network, where migration rates are independently updated at rate $\theta > 0$. Our results can be summarised in three observations. Firstly, the rate of speciation is higher in smaller populations, which is consistent with empirical evidence (see [32]). Secondly, upon a speciation event, there is typically a single population detaching from the mother species. Finally, we examined the relationship between the rate of environmental change and the rate of speciation, and found a non-trivial relationship between the two: at first glance, one could think that speciation rates decrease for lower values of θ (because the environment becomes increasingly stable), and that speciation is more frequent when the rate of environmental change is large. However, our observations suggest that this no longer holds when the rate of change becomes too large. Heuristically, this is due to the fact that in order to initiate a speciation event, geographic restrictions must be maintained for some time, allowing the positive feedback loop between genetic distance and effective migration rate to kick in. If migration rates are updated too quickly, the geographic restrictions nec-

essary for speciation disappear before significant divergence can occur.

Open questions and future work.

The numerical simulations of the stochastic model (see Fig. 2) revealed an intriguing behaviour of genetic proximities when the number of loci is small. In fact, speciation seems to result from stochastic fluctuations around the quasi-equilibrium of the genetic proximities. Thus, it would be interesting to study the deviations from the stochastic model, which could shed light on questions related to the average time to first speciation as a function of the number of loci considered.

Taking colonisation and extinction events into account could be an interesting addition to our model. On the one hand, this enables a more biologically realistic modelling of speciation. On the other hand, taking these events into account complicates the original dynamics of two opposing forces, raising interesting questions from a mathematical point of view.

In the framework of the model, a question of interest concerns the expected time to speciation of large meta-populations. Specifically, in Fig. 10, the left hand side suggests that the time to speciation increases very rapidly with the number of sub-populations. It would be interesting to find an expression of the rate of speciation as a function of the number of populations, that yields coherent results with empirical speciation rate differences as a function of population size (see [37]). Further, this raises the question of whether we can constrain the set of feedback functions that can be considered to model isolation regimes within a taxon by fitting the simulated increase in time to speciation associated to a feedback function to empirical data.

More generally, considering the observed significance of the feedback function, it is crucial to gain further insight into how to compute h in simple models of quantitative genetics, and how to infer it from experimental data. In particular, studies of speciation between diverging populations that continue to exchange genes could provide insight into this issue (see for example [4]). We believe that this would provide significant advances in our understanding of speciation rate variation, and take us a step closer to distinguishing the set of evolutionary forces that underlie species diversity.

References

- [1] M. Kopp, “Speciation and the neutral theory of biodiversity: Modes of speciation affect patterns of biodiversity in neutral communities,” Bioessays, vol. 32, no. 7, pp. 564–570, 2010.
- [2] D. E. Irwin, J. H. Irwin, and T. D. Price, “Ring species as bridges between microevolution and speciation,” Microevolution rate, pattern, process, pp. 223–243, 2001.
- [3] J. Coyne and H. Orr, Speciation. Speciation, Oxford University Press, Incorporated, 2004.
- [4] C. Roux, C. Fraisse, J. Romiguier, Y. Anciaux, N. Galtier, and N. Bierne, “Shedding light on the grey zone of speciation along a continuum of genomic divergence,” PLoS biology, vol. 14, no. 12, p. e2000234, 2016.
- [5] P. Nosil, “Speciation with gene flow could be common,” 2008.
- [6] S. Gavrillets, “Models of speciation: where are we now?,” Journal of heredity, vol. 105, no. S1, pp. 743–755, 2014.
- [7] P. G. Higgs and B. Derrida, “Stochastic models for species formation in evolving populations,” Journal of Physics A: Mathematical and General, vol. 24, no. 17, p. L985, 1991.
- [8] F. Manzo and L. Peliti, “Geographic speciation in the derrida-higgs model of species formation,” Journal of Physics A: Mathematical and General, vol. 27, no. 21, p. 7079, 1994.
- [9] S. Gavrillets, L. Hai, and M. D. Vose, “Rapid parapatric speciation on holey adaptive landscapes,” Proceedings of the Royal Society of London. Series B: Biological Sciences, vol. 265, no. 1405, pp. 1483–1489, 1998.
- [10] K. H. ten Tusscher and P. Hogeweg, “The role of genome and gene regulatory network canalization in the evolution of multi-trait polymorphisms and sympatric speciation,” BMC Evolutionary Biology, vol. 9, no. 1, pp. 1–21, 2009.
- [11] S. Gavrillets, “Waiting time to parapatric speciation,” Proceedings of the Royal Society of London. Series B: Biological Sciences, vol. 267, no. 1461, pp. 2483–2492, 2000.
- [12] É. Couvert, F. Bienvenu, J.-J. Duchamps, A. Erard, V. Miró Pina, E. Schertzer, and A. Lambert, “Opening the species box: what parsimonious microscopical models of speciation have to say about macroevolution,” Journal of Evolutionary Biology, vol. 37, no. 12, pp. 1433–1457, 2024.
- [13] P. Nosil and D. Schluter, “The genes underlying the process of speciation,” Trends in ecology & evolution, vol. 26, no. 4, pp. 160–167, 2011.
- [14] P. Nosil, J. L. Feder, S. M. Flaxman, and Z. Gompert, “Tipping points in the dynamics of speciation,” Nature Ecology & Evolution, vol. 1, no. 2, p. 0001, 2017.
- [15] V. M. Pina and E. Schertzer, “How does geographical distance translate into genetic distance?,” Stochastic Processes and their Applications, vol. 129, no. 10, pp. 3893–3921, 2019.
- [16] M. Sinitambirivoutin, P. Nosil, S. Flaxman, J. Feder, Z. Gompert, and V. Dakos, “Early-warning signals of impending speciation,” Evolution, vol. 77, no. 6, pp. 1444–1457, 2023.
- [17] S. Gavrillets, Fitness landscapes and the origin of species (MPB-41), vol. 88. Princeton University Press, 2018.
- [18] S. Gavrillets, R. Acton, and J. Gravner, “Dynamics of speciation and diversification in a metapopulation,” Evolution, vol. 54, no. 5, pp. 1493–1501, 2000.
- [19] D. M. McCandlish and A. Stoltzfus, “Modeling evolution using the probability of fixation: history and implications,” The Quarterly review of biology, vol. 89, no. 3, pp. 225–252, 2014.
- [20] Z. Patwa and L. M. Wahl, “The fixation probability of beneficial mutations,” Journal of The Royal Society Interface, vol. 5, no. 28, pp. 1279–1289, 2008.
- [21] M. Kimura, “On the probability of fixation of mutant genes in a population,” Genetics, vol. 47, no. 6, p. 713, 1962.
- [22] A. Etheridge, Some Mathematical Models from Population Genetics: École D’Été de Probabilités de Saint-Flour XXXIX-2009, vol. 2012. Springer Science & Business Media, 2011.
- [23] H. A. Orr, “The population genetics of speciation: the evolution of hybrid incompatibilities,” Genetics, vol. 139, no. 4, pp. 1805–1813, 1995.
- [24] N. H. Barton and G. M. Hewitt, “Adaptation, speciation and hybrid zones,” Nature, vol. 341, no. 6242, pp. 497–503, 1989.

- [25] S. R. Kuchta, D. S. Parks, R. L. Mueller, and D. B. Wake, “Closing the ring: historical biogeography of the salamander ring species *ensatina eschscholtzii*,” Journal of Biogeography, vol. 36, no. 5, pp. 982–995, 2009.
- [26] N. I. Cacho and D. A. Baum, “The caribbean slipper spurge *euphorbia tithymaloides*: the first example of a ring species in plants,” Proceedings of the Royal Society B: Biological Sciences, vol. 279, no. 1742, pp. 3377–3383, 2012.
- [27] N. Berestycki, “Mixing times of markov chains: Techniques and examples,” Alea-Latin American Journal of Probability and Mathematical Statistics, 2016.
- [28] D. Aldous and J. Fill, “Reversible markov chains and random walks on graphs,” 2002.
- [29] C. Cooper, R. Elsasser, H. Ono, and T. Radzik, “Coalescing random walks and voting on connected graphs,” SIAM Journal on Discrete Mathematics, vol. 27, no. 4, pp. 1748–1758, 2013.
- [30] S. Singhal, H. Huang, M. R. Grundle, M. R. Marchán-Rivadeneira, I. Holmes, P. O. Title, S. C. Donnellan, and D. L. Rabosky, “Does population structure predict the rate of speciation? a comparative test across australia’s most diverse vertebrate radiation,” The American Naturalist, vol. 192, no. 4, pp. 432–447, 2018.
- [31] S. Gavrillets, H. Li, and M. D. Vose, “Patterns of parapatric speciation,” Evolution, vol. 54, no. 4, pp. 1126–1134, 2000.
- [32] B. S. Khatri and R. A. Goldstein, “A coarse-grained biophysical model of sequence evolution and the population size dependence of the speciation rate,” Journal of theoretical biology, vol. 378, pp. 56–64, 2015.
- [33] S. P. Hubbell, The unified neutral theory of biodiversity and biogeography (MPB-32). Princeton University Press, 2011.
- [34] L. H. Rieseberg and J. H. Willis, “Plant speciation,” science, vol. 317, no. 5840, pp. 910–914, 2007.
- [35] J. D. Pongracz, D. Paetkau, M. Branigan, and E. Richardson, “Recent hybridization between a polar bear and grizzly bears in the canadian arctic,” Arctic, pp. 151–160, 2017.
- [36] J. Mallet, “Hybridization, ecological races and the nature of species: empirical evidence for the ease of speciation,” Philosophical Transactions of the Royal Society B: Biological Sciences, vol. 363, no. 1506, pp. 2971–2986, 2008.
- [37] A. M. Makarieva and V. G. Gorshkov, “On the dependence of speciation rates on species abundance and characteristic population size,” Journal of Biosciences, vol. 29, pp. 119–128, 2004.
- [38] N. Fournier and S. Méléard, “A microscopic probabilistic description of a locally regulated population and macroscopic approximations,” 2004.
- [39] P. Billingsley, Convergence of probability measures. John Wiley & Sons, 2013.
- [40] A. V. Skorokhod, “Limit theorems for stochastic processes,” Theory of Probability & Its Applications, vol. 1, no. 3, pp. 261–290, 1956.
- [41] D. Aldous, “Stopping times and tightness,” The Annals of Probability, pp. 335–340, 1978.
- [42] R. Rebolledo, “Central limit theorems for local martingales,” Zeitschrift für Wahrscheinlichkeitstheorie und verwandte Gebiete, vol. 51, no. 3, pp. 269–286, 1980.
- [43] B. A. Neumann, “Nonlinear markov chains with finite state space: Invariant distributions and long-term behaviour,” Journal of Applied Probability, vol. 60, no. 1, pp. 30–44, 2023.
- [44] D. W. Stroock, An introduction to Markov processes, vol. 230. Springer Science & Business Media, 2013.

Appendices

A Deriving the master equation

This section is devoted to the derivation of the master equation (3). The key idea is that we can represent the state and transitions of the model with the help of partitions in a Markov way. In fact, we are less interested in the alleles themselves than in their different realisations between populations, and thus, we will divide the populations at each locus into blocks - depending on which other populations they share the same allele with. The mathematical equivalent of this idea are partitions: for any $n \in \mathbb{N}$, we define $[n] := \{1, \dots, n\}$, and denote the set of partitions of $[n]$ with \mathcal{P}_n . We denote by B_n the cardinal of \mathcal{P}_n (Bell's number).

To rigorously define our process, we need to introduce some notation. Let $K \in [L]$ be a given locus, and $i, j \in [N]$ two populations, with $L, N \in \mathbb{N}$. We define the equivalence relation \sim w.r.t. to a partition $\pi \in \mathcal{P}_N$ (and at a locus K) as

$$i \sim_{\pi} j \quad :\Leftrightarrow \quad \exists A \in \pi : i, j \in A.$$

Hence, we have $i \sim_{\pi} j$ if there is a block in π such that i and j are in the same block. Then, we say that the **allelic partition** at a given locus $K \in [L]$ is given by $\pi \in \mathcal{P}_N$, if the blocks of π correspond to the equivalence classes of \sim_{π} at locus K . This is a simple way to study genetic differences between populations, because we actually do not have to keep record of any allele, or, speaking in terms of Fig. 1, we do not have to keep using different colours to distinguish differences in genetic material.

We now define the stochastic processes we will be interested in. The process of **allelic partitions**

$$(\vec{\Pi}_t^{(L)})_{t \geq 0} := (\vec{\Pi}_t)_{t \geq 0} = (\Pi_t^1, \dots, \Pi_t^L)_{t \geq 0}$$

is valued in $\mathcal{P}_N^{\otimes L}$, and for every $K \in [L]$, we think of $\Pi_t^K \in \mathcal{P}_N$ as the allelic partition at locus K at time $t > 0$. Finally, to compute the genetic proximity between two populations at time t from the process $(\vec{\Pi}_t)_{t \geq 0}$, we define two functions. We set, for all $\pi \in \mathcal{P}_N, \vec{\sigma} \in \mathcal{P}_N^{\otimes L}$, and all populations $i, j \in [N]$,

$$f_{\pi}(\vec{\sigma}) := \frac{1}{L} \sum_{K=1}^L \mathbf{1}_{\{\sigma_K = \pi\}}, \quad (15)$$

and

$$p_{ij}^{(L)}(\vec{\sigma}) := \frac{1}{L} \sum_{K=1}^L \mathbf{1}_{\{i \sim_{\sigma_K} j\}}. \quad (16)$$

Intuitively, $f_{\pi}(\vec{\Pi}_t)$ will correspond to the fraction of loci with an allelic partition π , whereas $p_{ij}^{(L)}(t) := p_{ij}^{(L)}(\vec{\Pi}_t)$ will correspond to the **genetic proximity** between island i and j at time t . Note that this definition is just the mathematical translation of the above idea of counting the number of different alleles.

The process $(\vec{\Pi}_t)_{t \geq 0}$, and thus the process of genetic proximities $\{(p_{ij}^{(L)}(t))_{t \geq 0} : i, j \in [N]\}$, will be governed by two antagonist forces:

1. **Mutation events:** within each sub-population i , at each locus K and at a constant rate μ , mutation occurs. Given a mutation event, the allelic partition Π_t^K changes to $s_i(\Pi_t^K)$, the partition created from Π_t^K by isolating the singleton i into a block of its own.
2. **Migration events:** between every sub-population i and j , at each locus K , migration events occur at an effective rate

$$m_{ij}^e = m_{ij} \cdot h(p_{ij}^{(L)}(\vec{\Pi}_t)), \quad (17)$$

We refer to page 3 for the definitions of m_{ij} and h . Given a migration event from i to j , the allelic partition Π_t^K at locus K changes to $\sigma_{j \rightarrow i}(\Pi_t^K)$, the partition created from Π_t^K by putting the element j in the block containing i . Heuristically, when i migrates to j , the element j will take the type of i , which corresponds to placing j into the block containing i .

We devote this Section to a mathematically rigorous proof of the convergence of our stochastic model to the master equation. In other words, we will describe a deterministic limit for the process $(\vec{\Pi}_t; t \geq 0)$ as the number of loci L does to infinity. We will achieve this by deriving a law of large numbers using classical martingale theory, see e.g. [38].

To expose the main result of the section, we start with some notations. Set

$$\mathcal{M}_1(\mathcal{P}_N) := \left\{ \vec{\rho} = (\rho_\pi)_{\pi \in \mathcal{P}_N}, \quad \sum_{\pi \in \mathcal{P}_N} \rho_\pi = 1 \right\}$$

the set of probability measures on \mathcal{P}_N . For every $\vec{\rho} \in \mathcal{M}(\mathcal{P}_N)$, we set $\vec{\rho}(i \sim j) := \sum_{\pi: i \sim j} \rho_\pi$. Finally, $A(\vec{\rho})$ is the transition rate matrix such that for $\pi \neq \pi'$

- $A_{\pi, \pi'}(\vec{\rho}) = \mu$, if $\pi' = s_i(\pi)$ for some $i \in [N]$
- $A_{\pi, \pi'}(\vec{\rho}) = m_{ij}h \left(\vec{\rho}(i \sim j) \right)$, if $\pi' = \sigma_{j \rightarrow i}(\pi)$ for some $i, j \in [N]$.

Define

$$\forall \pi \in \mathcal{P}_N, \quad X_\pi^{(L)}(t) := f_\pi(\vec{\Pi}_t) = \frac{1}{L} \sum_{K=1}^L \mathbf{1}_{\{\Pi_t^K = \pi\}} \quad (18)$$

and $\vec{X}^{(L)} \equiv \vec{X} = (X_\pi)_{\pi \in \mathcal{P}_N}$ the process in \mathbb{D} , the space of càdlàg functions valued in $\mathcal{M}_1(\mathcal{P}_N)$ endowed with the Skorohod (J1)-topology [39, 40]. The following section will be dedicated to the proof of the following result.

Theorem A.1 *The sequence $(\vec{X}^{(L)})_L$ converges in law to $(\vec{x}(t))_{t \geq 0} = ((x_\pi(t))_{\pi \in \mathcal{P}_N})_{t \geq 0}$, the unique solution of the deterministic ODE*

$$\frac{d\vec{x}(t)}{dt} = \vec{x}(t)A(\vec{x}(t)) =: \vec{F}(\vec{x}(t)) \quad (19)$$

We decompose the proof into several elementary lemmas. The first lemma is obtained by straight-forward computations, and thus we omit the proof.

Lemma A.2 *Let $Q^{(L)}$ be the generator of the partition process $(\vec{\Pi}_t)_{t \geq 0}$. Then*

$$Q^{(L)} \vec{f}(\nu) = \vec{f}(\nu)A(\vec{f}(\nu)), \quad (20)$$

for all $\vec{f}: \mathcal{P}_N^{\otimes L} \rightarrow \mathbb{R}, \nu \in \mathcal{P}_N^{\otimes L}$.

Lemma A.3 *Define*

$$\begin{aligned} M_\pi^{(L)}(t) &:= f_\pi(\vec{\Pi}_t) - f_\pi(\vec{\Pi}_0) - \int_0^t Q^{(L)} f_\pi(\vec{\Pi}_u) du. \\ &= X_\pi(t) - X_\pi(0) - \int_0^t \left(\vec{F}(\vec{X}(t)) \right)_\pi du. \end{aligned}$$

Then, the quadratic variation of the martingale M_π verifies

$$\langle M_\pi^{(L)} \rangle_t = O\left(\frac{1}{L}\right) \quad \text{as } L \rightarrow \infty.$$

Proof For any $\rho \in \mathcal{P}_N^{\otimes L}$, we denote by $\rho_{K, \pi'}$ the partition vector obtained from ρ by changing the K -th coordinate of ρ to the partition π' . Additionally, we denote by $\tau(\rho, \rho')$, for any $\rho, \rho' \in \mathcal{P}_N^{\otimes L}$, the rate of change from ρ to ρ' . The quadratic variation of M^L is given by

$$\langle M_\pi^L \rangle_t = \int_0^t \sum_{K=1}^L \sum_{\pi' \neq (\Pi_u)_K} (f_\pi((\Pi_u)_{K, \pi'}) - f_\pi(\Pi_u))^2 \cdot \tau((\Pi_u), (\Pi_u)_{K, \pi'}) du.$$

On the one hand, $(f_\pi((\Pi_u)_{K,\pi'}) - f_\pi(\Pi_u))^2 \leq \frac{1}{L^2}$. On the other hand, the rates can be uniformly bounded in L by $0 < \tau_{\max} < \infty$. This yields

$$\langle M_\pi^L \rangle_t \leq \frac{t B_N \tau_{\max}}{L}. \quad (21)$$

□

Lemma A.4 *The sequence $\{(\vec{X}^L(t))_{t \geq 0}\}_{L \in \mathbb{N}}$ is tight in \mathbb{D} .*

Proof We will use the Aldous-Rebolledo criterion for tightness, see [41, 42]. To prove tightness of \vec{X}^L , it suffices to prove tightness of each coordinate.

Denote \mathbb{F}_L the natural filtration of the \mathbb{D} valued process \vec{X}^L . Let S, S' two stopping times w.r.t. \mathbb{F}_L such that $0 \leq S \leq S' \leq S + \delta \leq T$ for $T \in \mathbb{R}_+$ and $\delta > 0$. Let $\pi \in \mathcal{P}_N$. Remark that

$$X_\pi^L(S') - X_\pi^L(S) = M_\pi^L(S') - M_\pi^L(S) + \int_S^{S'} Q^L f_\pi(\vec{\Pi}_u) du.$$

We have to prove that the laws of the martingale part and of the finite variation part are tight. Using that M_π^L is a martingale and the monotony of the quadratic variation, we get

$$\begin{aligned} \mathbb{E}(|M_\pi^L(S') - M_\pi^L(S)|^2) &\leq \mathbb{E}(M_\pi^L(S')^2 - M_\pi^L(S)^2) \\ &\leq \mathbb{E}(\langle M_\pi^L \rangle_{S+\delta} - \langle M_\pi^L \rangle_S) \\ (21) \quad &\leq \frac{B_N \tau_{\max}}{L} \mathbb{E} \left(\int_S^{S+\delta} du \right) \leq B_N \tau_{\max} \delta, \end{aligned}$$

which allows us to deduce tightness of the martingale part. It remains to prove tightness of the finite variation part. This can be seen directly by the same argument and the uniform boundedness in L of the generator. □

Proof [Proof of Theorem A.1] Because h and \vec{F} are \mathcal{C}^1 functions, there exists a unique solution to the deterministic master equation (19) by standard Cauchy-Lipschitz arguments. By Lemma A.4 and an application of Prohorov's and Skorohod's theorems, there exists a subsequential limit of the sequence $(\vec{X}^{(L)})$, which we will denote \vec{X}^∞ . Let us show that any subsequential limit of \vec{X}^∞ is solution to the equation (19).

Let $t > 0$, and recall that

$$M_\pi^L(t) = X_\pi^L(t) - X_\pi^L(0) - \int_0^t \left(\vec{F}(\vec{X}^L(u)) \right)_\pi du.$$

On the one hand, Lemma A.3 yields

$$\mathbb{E}[(M_\pi^L(t))^2] \rightarrow 0, \quad \text{as } L \rightarrow \infty,$$

which in particular implies

$$\mathbb{E} \left(\int_0^t \left(X_\pi^L(s) - X_\pi^L(0) - \int_0^s \left(\vec{F}(\vec{X}^L(u)) \right)_\pi du \right)^2 ds \right) \rightarrow 0, \quad (22)$$

as $L \rightarrow \infty$. On the other hand, as \vec{X}^L converges to \vec{X}^∞ in a weak sense, we know that the set of discontinuities of \vec{X}^∞ has Lebesgue measure 0, and since the \vec{X}^L are uniformly bounded,

$$\int_0^t M_\pi^L(s) ds \rightarrow \int_0^t X_\pi^\infty(s) - X_\pi^\infty(0) - \int_0^s \left(\vec{F}(\vec{X}^\infty(u)) \right)_\pi du ds,$$

as $L \rightarrow \infty$. Thus, taking expectations and using (22) allows us to conclude that a.s.,

$$X_\pi^\infty(t) - X_\pi^\infty(0) - \int_0^t \left(\vec{F}(\vec{X}^\infty(u)) \right)_\pi du = 0. \quad (23)$$

□

B Duality

Since the dimension of the master equation (19) is the number of partitions of the set $[N] = \{1, \dots, N\}$, the ODE system quickly becomes intractable. Thus, we will prove a duality relation allowing us to reduce the dimension of the system of interest to $N(N-1)/2$, the number of pairs of $[N]$.

The main idea relies on a stochastic interpretation of the master equation (19). To gain some intuition, we first recall the definition of the Moran model with mutation on a directed weighted graph. Consider a population of individuals $1, \dots, N$ and a dynamical matrix $(M_{ij}(t))_{t \geq 0, i \neq j \in [N]}$ with non-negative entries. The system evolves according to the following dynamics.

- Each individual takes on a new type at rate μ (infinite allele assumption).
- For $i \neq j$ and at time t , individual j takes on the type of individual i at rate $M_{ij}(t)$.

As before, we can conveniently encode the dynamics by recording the allelic partition along time. This defines a time-inhomogeneous Markov process valued in \mathcal{P}_N .

Let us now introduce the nonlinear Markov process version of the latter Moran model. Informally, this amounts to assuming that the dynamical migration matrix $M(t)$ depends on the law of the process itself; namely, we consider the partition process $(\sigma_t; t \geq 0)$ on \mathcal{P}_N induced by a time-inhomogeneous Moran model with dynamical matrix

$$\forall i \neq j \in [N], \quad M_{ij}(t) = m_{ij} h(\hat{p}_{ij}(t)) \quad \text{where } \hat{p}_{ij}(t) := \mathbb{P}(i \sim_{\sigma_t} j). \quad (24)$$

Following the terminology of [43], $(\sigma_t)_{t \geq 0}$ defines a finite-state time-inhomogeneous Markov chain whose semi-group is determined by the solution to a non-linear differential forward Kolomogorov equation.

More formally, let $s > 0$. It is clear by the definition of $M(s)$ that at time s , the transition rate matrix of the partition-valued process $(\sigma_t; t \geq 0)$ is given by $A(\vec{p}_s)$, where

$$\vec{p}_s = (\mathbb{P}(\sigma_s = \pi))_{\pi \in \mathcal{P}_N},$$

and A is given in Appendix A. We note that the application $p \mapsto A(p)$ is a Lipschitz continuous and bounded function. By Theorem 2.1 in [43], there exists a unique (time-inhomogeneous) Markov process $(\sigma_t)_{t \geq 0}$ valued in \mathcal{P}_N , whose semi-group $(S(t))_{t \geq 0}$ is characterized by the non-linear forward Kolmogorov equation

$$\frac{dS(t)}{dt} = S(t)A(S(t)). \quad (25)$$

In particular, we recover the limiting master equation (19) for each coordinate of the matrix equation, i.e., for the functions

$$t \mapsto \mathbb{P}_{\pi, \pi'}(t) = \mathbb{P}_{\pi}(\sigma_t = \pi').$$

This justifies the interpretation of $\hat{p}_{ij}(t)$ (see (24)) as the genetic proximity introduced in Section 2 between populations i and j , in the large loci regime.

As in the standard Moran model [22], we consider the following graphical representation on $[N] \times \mathbb{R}_+$:

- For a reproductive event $i \rightarrow j$ at time t , draw an arrow with tail at (i, t) and tip at (j, t)
- For a mutation event at site k at time t , draw a \star at (k, t) .

Via the graphical representation we discussed in section 3, (see Fig. 3), we can associate to every individual an ancestral lineage using the arrow-star configuration. For every point (i, t) with $i \in [N]$, we define $S_{(i, t)}$ to be the ancestral lineage starting from (i, t) . The system of ancestral lineages $(S^{(1, t)}(s), \dots, S^{(N, t)}(s); s \leq t)$ starting from time horizon $t > 0$ evolves according to the following dynamics.

- Lineages are running backward in time and evolve independently until they coalesce.
- A lineage jumps from j to i at time s at rate $m_{ij} h(p_{ij}(t-s))$.
- A lineage is killed (or stopped) at rate μ .

We can recover the allelic partition from these ancestral lineages by remarking that two individuals i, j are in the same block at time t iff the ancestral lineages $S_{(i,t)}$ and $S_{(j,t)}$ trace back to the same type. In turn, the lineages trace back to the same type if one of two events happen: (1) The two lineages $S_{(i,t)}, S_{(j,t)}$ coalesce before time t ; or (2) the two lineages survive up to time t , they do not coalesce, but they hit two sites in the same partition, i.e., if there are i_0, j_0 such that $S_{(i,t)}(t) = (i_0, 0)$ and $S_{(j,t)}(t) = (j_0, 0)$ for some $i_0 \neq j_0 \in [N]$, such that $i_0 \sim_{\sigma_0} j_0$. This leads to the following proposition.

Proposition B.1 *Consider the unkilld ancestral lineages $\bar{S}_{(i,t)}$ and $\bar{S}_{(j,t)}$, i.e., the ancestral lineages starting from (i, t) and (j, t) and ignoring the killing event \star . (Equivalently, this amounts to set $\mu = 0$). Define the coalescing time*

$$T_{(i,j),t} := \sup\{u > 0 : \bar{S}_{(i,t)}(u) = \bar{S}_{(j,t)}(u)\}.$$

If

$$p_{ij}(t) = \mathbb{P}(i \sim_{\sigma_t} j),$$

then

$$p_{ij}(t) = \mathbb{E}(e^{-2\mu T_{(i,j),t}}; T_{(i,j),t} \leq t) + \mathbb{E}(e^{-2\mu T_{(i,j),t}}; \bar{S}_{(i,t)}(t) \sim_{\sigma_0} \bar{S}_{(j,t)}(t), T_{(i,j),t} > t). \quad (26)$$

With the help of Proposition B.1, we can establish an ODE system for the genetic proximities.

Corollary B.2 *The genetic proximities p_{ij} solve the following system of ordinary differential equations,*

$$\begin{aligned} \frac{dp_{ij}}{dt}(t) &= \sum_{k=1}^N (m_{ik}h(p_{ik}(t))p_{kj}(t) + m_{jk}h(p_{jk}(t))p_{ik}(t)) \\ &\quad - p_{ij}(t) \left(\sum_{k=1}^N (m_{ik}h(p_{ik}(t)) + m_{jk}h(p_{jk}(t))) + 2\mu \right), \end{aligned} \quad (27)$$

where we set $m_{kk} = 0$ and $p_{kk}(t) = 1$ for all k .

Proof We will only show the result where the initial condition is given by the singleton partition. The general case can be proved along the same lines.

We will use Proposition B.1, and condition the expected value on the possible jumps of the unkilld random walks $S_i := \bar{S}_{(i,t)}$ and $S_j := \bar{S}_{(j,t)}$ in a small interval of time of length $dt > 0$. Then,

$$\begin{aligned} p_{ij}(t) &= \mathbb{E}(\mathbb{E}(e^{-2\mu T_{(i,j),t}} \mathbf{1}_{\{T_{(i,j),t} \leq t\}} | (S_i(u))_{u \in [0, dt]}, (S_j(u))_{u \in [0, dt]})) \\ &= \Delta_0(dt) + \Delta_{1,i}(dt) + \Delta_{1,j}(dt) + \Delta_2(dt), \end{aligned}$$

where Δ_0 corresponds to the case where neither random walk jumps, $\Delta_{1,k}$ to the case where the process starting from $k \in \{i, j\}$ jumps and the last quantity for the case where there are at least two jumps. The last quantity will be of order dt^2 , and hence disappear in the limit when we divide by dt .

Case 1: S_i jumps once.

Case 1.1: S_i jumps to $k \neq j$. Denote the number of jumps of the process (S_i, S_j) in the time interval $[0, s]$, where $0 < s \leq t$, as $\mathcal{N}([0, s]) = (\mathcal{N}_i([0, s]), \mathcal{N}_j([0, s]))$, and let $k \neq j$. Then, define

$$A_{i \rightarrow k, dt} = \{dt < T_{(i,j),t} \leq t\} \cap \{\mathcal{N}([0, dt]) = (1, 0), S_i(dt) = k\},$$

On this event, we have

$$T_{(i,j),t} = T_{(k,j),t-dt} + dt.$$

The probability that the random walk starting from i jumps exactly once on the interval $[0, dt]$ to location k is given by

$$m_{ik}h(p_{ik}(t)) \cdot dt + o(dt),$$

which follows with the continuity of the function $h \circ p_{ik}$.

Case 1.2: S_i jumps to j . We consider the event where coalescence happens on the time interval $[0, dt]$. The corresponding probability is given by

$$m_{ij}h(p_{ij}(t)) \cdot dt + o(dt),$$

and the coalescence time $T_{(i,j),t}$ equals the jump time.

Putting cases 1.1 and 1.2 together, we obtain

$$\begin{aligned}\Delta_{1,i} &= dt \sum_{k \neq j} m_{ik} h(p_{ik}(t)) \mathbb{E}(e^{-2\mu(T_{(k,j),t-dt} + dt)} \mathbf{1}_{\{T_{(k,j),t-dt} \leq t-dt\}}) \\ &+ dt \cdot m_{ij} h(p_{ij}(t)) + o(dt).\end{aligned}$$

Since the probability to see an event in a time interval of length dt converges to zero, we get

$$\mathbb{E}(e^{-2\mu(T_{(k,j),t-dt} + dt)} \mathbf{1}_{\{T_{(k,j),t-dt} \leq t-dt\}}) = \mathbb{E}(e^{-2\mu T_{(k,j),t}} \mathbf{1}_{\{T_{(k,j),t} \leq t\}}) + o(1) = p_{kj}(t) + o(1),$$

and thus

$$\frac{\Delta_{1,i}(dt)}{dt} \xrightarrow{dt \rightarrow 0} \sum_{k \neq j} m_{ik} h(p_{ik}(t)) p_{kj}(t) + m_{ij} h(p_{ij}(t)).$$

Case 2: S_j jumps once. The same arguments as in case 1 can be applied.

Case 3: Neither S_i , nor S_j jump. We remark that conditionally on the event $A_0 = \{\mathcal{N}([0, dt]) = (0, 0)\}$, the coalescence time is given by

$$T_{(i,j),t} = T_{(i,j),t-dt} + dt.$$

Hence,

$$\Delta_0 = \left(1 - dt \cdot \left(\sum_{k=1}^N m_{ik} h(p_{ik}(t)) + m_{jk} h(p_{jk}(t))\right) + o(dt)\right) \cdot p_{ij}(t-dt) e^{-2\mu dt}.$$

Finally, we obtain

$$\begin{aligned}\lim_{dt \downarrow 0} \frac{p_{ij}(t+dt) - p_{ij}(t)}{dt} &= \sum_{k=1}^N (m_{ik} h(p_{ik}(t)) p_{kj}(t) + m_{jk} h(p_{jk}(t)) p_{ik}(t)) \\ &- \left(\sum_{k=1}^N (m_{ik} h(p_{ik}(t)) + m_{jk} h(p_{jk}(t))) + 2\mu\right) \cdot p_{ij}(t),\end{aligned}$$

which yields the desired result. \square

Consider a solution $\vec{p} = (p_{ij})_{i \neq j}$ to the system $\vec{F}(\vec{p}) = 0$. We recall that \vec{F} is given by

$$\vec{F}(p)_{ij} = \sum_{k=1}^N (m_{ik} h(p_{ik}) p_{kj} + m_{jk} h(p_{jk}) p_{ik}) - p_{ij} \left(\sum_{k=1}^N (m_{ik} h(p_{ik}) + m_{jk} h(p_{jk})) + 2\mu\right),$$

and the elements of the Jacobian by

$$\frac{\partial \vec{F}(p)_{ij}}{\partial p_{ij}} = (m_{ij} + m_{ji}) h'(p_{ij}) (1 - p_{ij}) - \left(\sum_{k=1}^N (m_{ik} h(p_{ik}) + m_{jk} h(p_{jk})) + 2\mu\right)$$

on the diagonal, and for $k \neq i, j$,

$$\frac{\partial \vec{F}(p)_{ij}}{\partial p_{ik}} = m_{ik} h'(p_{ik}) p_{kj} + m_{jk} h(p_{jk}) - p_{ij} m_{ik} h'(p_{ik})$$

for the cross terms.

C Results

Let $\vec{p} = (p_{ij})_{i \neq j}$ with entries in $[0, 1]$ (we think of p_{ij} as the genetic proximity between i and j at equilibrium). We start with some definitions.

C.1 General results

Definition C.1 Let G be an undirected, unweighted graph with vertices $[N]$, and $M = ((m_{ij})_{i,j \in [N]})$ a migration graph. We define the **modified migration matrix** $M(G) = (M(G)_{ij})_{i \neq j}$ as

$$M(G)_{ij} = \begin{cases} m_{ij} & \text{if } i \sim_G j \\ 0 & \text{otherwise} \end{cases},$$

where $i \sim_G j$ iff i and j are connected in G . Furthermore, we define the **species graph** $G(P^{eq})$ associated to an equilibrium as the undirected, unweighted graph with vertices $[N]$ and edges between any i and j such that $h(P_{ij}^{eq}) > 0$. Finally, we will use \sim_s as a short notation for the relation $\sim_{G(P^{eq})}$.

Theorem C.2 (Fixed Point Problem) Let $P^{eq} = (P_{ij}^{eq})_{i \neq j}$ be an equilibrium for the system of genetic proximities (27). Consider the unkilld ancestral lineages \bar{S}_i resp. \bar{S}_j starting from i resp. j on the species graph $G_{P^{eq}}$, i.e., with jump rates given by its weighted edges. Define the coalescing time

$$T_{ij} := \inf\{u > 0 : \bar{S}_i(u) = \bar{S}_j(u)\}.$$

Then, P^{eq} satisfies the fixed point problem

$$P_{ij}^{eq} = \mathbb{E} \left(e^{-2\mu T_{ij}(P^{eq})} \right) \quad (28)$$

Proof The proof easily follows from (26) by letting $t \rightarrow \infty$. \square

In the following proposition, we show that species graphs are transitive, if the feedback function does not have a threshold.

Proposition C.3 Assume that h verifies $h(x) > 0$ for all $x \in (0, 1)$. Then, the corresponding species is transitive.

Proof Let i, j and k such that $h(P_{ik}^{eq}), h(P_{jk}^{eq}) > 0$. We have to show that $h(P_{ij}^{eq}) > 0$. We have $T_{i,j} < \infty$ a.s. The result follows directly by the relation (28), which we obtain from the previous proposition. \square

Theorem C.4 Let $P^{eq} = (P_{ij}^{eq})_{i \neq j}$ an equilibrium for the system of genetic proximities (27), and $\Pi(P^{eq})$ the induced equilibrium for the master equation (19). Then, P^{eq} is stable for (27) iff $\Pi(P^{eq})$ is stable for (19).

Proof Follows directly from Proposition B.1. \square

Proposition C.5 Assume that h verifies $h'(0) = 0$. Let $P^{eq} = (P_{ij}^{eq})_{i \neq j}$ an equilibrium for the system of genetic proximities (27). Let $G = G(P^{eq})$ be the species graph of P^{eq} , and let $M(G)$ the modified migration matrix w.r.t. the species graph of P^{eq} . Then,

1. P^{eq} is an equilibrium for the modified migration matrix.
2. P^{eq} is (locally) stable for the modified dynamics iff it is (locally) stable for the original dynamics.

Proof We write \vec{F}_M respectively $\vec{F}_{M(G)}$ to indicate the dependency of \vec{F} on the migration rates. The first point is a direct consequence of (28). To address the second point, we only need to ensure that the entries of the Jacobians $J_{\vec{F}_M}(P^{eq})$ and $J_{\vec{F}_{M(G)}}(P^{eq})$ coincide. This follows from the fact that if i and j are not connected in the species graph G , then $P_{ij}^{eq} = 0$. Since m_{ij} appears only in a product with $h(P_{ij}^{eq})$ or $h'(P_{ij}^{eq})$, we use the definition of $M(G)$ and the assumptions on h to conclude. \square

Proposition C.6 Assume that h verifies $h'(0) = 0$. Let $P^{eq} = (P_{ij}^{eq})_{i \neq j}$ an equilibrium for the system of genetic proximities (27). Then, the stability of P^{eq} is equivalent to the stability of each species of $G(P^{eq})$. More precisely, P^{eq} is (locally) stable iff for every connected component $S = (V, A)$ of $G(P^{eq})$, the modified equilibrium $\vec{p}_{e,S}$ given by

$$p_{ij}^{e,S} = \mathbf{1}_{\{(i,j) \in S\}} \cdot P_{ij}^{eq},$$

is such that for every eigenvalue λ of the Jacobian $J(\vec{p}_{e,S})$, we have $\text{Re}(\lambda) < 0$.

Proof We set

$$E_{\sim} := \{\vec{y} = (y_{ij})_{i \neq j} : y_{kl} = 0 \text{ if } k \sim_s l\}$$

and

$$E_{\not\sim} := \{\vec{y} = (y_{ij})_{i \neq j} : y_{kl} = 0 \text{ if } k \not\sim_s l\}.$$

We want to show that the stability of $J := J_{\vec{F}}(P^{\text{eq}})$ is equivalent to the stability of J restraint to E^* . Let us first show that J verifies $J(E_{\sim}) \subset E_{\sim}$ and $J(E_{\not\sim}) \subset E_{\not\sim}$, which yields the decomposition of the eigenvalues of J in terms of the eigenvalues restraint to E_{\sim} respectively E^* . Let $\vec{y} \in E_{\sim}$, and i, j such that $i \sim_s j$. We have

$$(J \cdot y)_{ij} = \sum_{(k,l)} J_{(ij),(kl)} y_{kl} = \sum_{(k,l): k \not\sim_s l} J_{(ij),(kl)} y_{kl},$$

where we used the definition of E_{\sim} . Hence, let us compute $\frac{\partial \vec{F}(P^{\text{eq}})_{ij}}{\partial p_{ik}}$, for k and i such that $i \not\sim_s k$. Since \sim_s is transitive on $G(P^{\text{eq}})$, we have $j \not\sim_s k$. Thus,

$$\frac{\partial \vec{F}(P^{\text{eq}})_{ij}}{\partial p_{ik}} = m_{ik} h'(P_{ik}^{\text{eq}})(P_{kj}^{\text{eq}} - P_{ij}^{\text{eq}}) + m_{jk} h(P_{jk}^{\text{eq}}) = 0,$$

since h verifies $h'(0) = 0$. Thus $J(E_{\sim}) \subset E_{\sim}$. Let now $\vec{y} \in E_{\not\sim}$, and i, j such that $i \not\sim_s j$. We have

$$(J \cdot y)_{ij} = \sum_{(k,l)} J_{(ij),(kl)} y_{kl} = \sum_{(k,l): k \sim_s l} J_{(ij),(kl)} y_{kl}.$$

Let k such that $i \sim_s k$. Transitivity of \sim_s yields $j \not\sim_s k$, and thus $P_{ij}^{\text{eq}} = P_{jk}^{\text{eq}} = 0$. Thus $J_{(ij),(ik)} = 0$, and therefore $J(E_{\not\sim}) \subset E_{\not\sim}$, which yields (why?)

$$\text{Sp}(J) = \text{Sp}(J|_{E_{\sim}}) \cup \text{Sp}(J|_{E_{\not\sim}}).$$

It remains to show that for all $\lambda \in \text{Sp}(J|_{E_{\sim}})$, $\text{Re}(\lambda) < 0$.

The computations above for $J|_{E_{\sim}} \cdot x$ for a vector $x \in E_{\sim}$ show that

$$(J|_{E_{\sim}})_{(ij),(ik)} = \mathbf{1}_{\{i \not\sim_s j, i \not\sim_s k, j \sim_s k\}} m_{jk} h(P_{jk}^{\text{eq}}).$$

It remains to compute the terms on the diagonal, which can be seen to equal

$$-2\mu - \left(\sum_{l \sim i} m_{il} h(P_{il}^{\text{eq}}) \right) - \left(\sum_{l \sim j} m_{jl} h(P_{jl}^{\text{eq}}) \right)$$

for all i, j such that $i \not\sim_s j$. From here, it is easy to see that we may write

$$J|_{E_{\sim}} = (-2\mu) \cdot \mathbf{I} + U,$$

where U is a transition rate matrix, and \mathbf{I} is the identity matrix. It is known (see, for instance, [44]), that the largest eigenvalue of U is given by 0, thus the stability of $J|_{E_{\sim}}$. This allows us to conclude. \square

Proposition C.7 (Stability characterisation for dust) *Let $M = ([N], (m_{ij})_{i \neq j})$ be a migration graph. Then, $\vec{p} = \mathbf{0}$ is an equilibrium for the system of genetic proximities (27). Additionally, it is a (locally) stable equilibrium iff*

$$\forall i, j, \quad h'(0) - \frac{2\mu}{m_{ji} + m_{ij}} < 0.$$

Proof The off-diagonal terms of the Jacobian $J_{\vec{F}}(0)$ all equal zero, and the diagonal terms are equal to $(m_{ij} + m_{ji})h'(0) - 2\mu$. The stability condition follows. \square

C.2 Stability and symmetry breaking in symmetric migration

Proposition C.8 (Stability of symmetric equilibria) *Let $M = ([N], (m_{ij})_{i \neq j})$ be a migration graph such that $m_{ij} = m > 0$ for all $i \neq j$, and $P^{eq} = (P_{ij}^{eq})_{i \neq j}$ a symmetric equilibrium for the system of genetic proximities (27), i.e., verifying $P_{ij}^{eq} = P^{eq} > 0$ for all $i \neq j$. Then,*

1. P^{eq} is solution to the equation

$$\varphi(P^{eq}) = h(P^{eq})(1 - P^{eq}) - \frac{\mu}{m}P^{eq} = 0 \quad (29)$$

2. P^{eq} is (locally) stable iff

$$\varphi'(P^{eq}) = h'(P^{eq})(1 - P^{eq}) - h(P^{eq}) - \frac{\mu}{m} < 0 \quad (30)$$

Proof From (27), we obtain that any symmetric equilibrium verifies

$$0 = 2mh(P^{eq})(1 - P^{eq}) + 2(N - 2)mh(P^{eq})P^{eq} - P^{eq}(2(N - 2)mh(P^{eq}) - 2\mu)$$

Thus the first statement.

The Jacobian $J := J_{\vec{F}}(P^{eq})$ of \vec{F} can be computed to

$$\frac{\partial \vec{F}(P^{eq})_{ij}}{\partial p_{ij}} = 2mh'(P^{eq})(1 - P^{eq}) - 2(N - 1)mh(P^{eq}) - 2\mu,$$

for the diagonal terms, and

$$\frac{\partial \vec{F}(P^{eq})_{ij}}{\partial p_{ik}} = mh(P^{eq}),$$

if $k \neq i, j$. Finally, $\frac{\partial \vec{F}(P^{eq})_{ij}}{\partial p_{kl}} = 0$ otherwise. In particular, we remark that we can write

$$J = 2m\varphi'(P^{eq}) \cdot \mathbf{I} + A,$$

where A is a transition rate matrix. Again, it is known (see, for instance, [44]), that the largest eigenvalue of A is given by 0. The stability condition follows. \square

To study the occurrence of asymmetric equilibria in symmetric migration, we start by considering a case where $[N]$ is split into two sets of vertices V_1 and V_2 . We then consider equilibria P^{eq} with three degrees of freedom, namely, the genetic proximity within V_1 (denoted by p_1), the genetic proximity within V_2 (denoted by p_2), and the genetic proximity between V_1 and V_2 (denoted by p_{inter}).

Proposition C.9 (Symmetry breaking I) *Let $M = ([N], (m_{ij})_{i \neq j})$ be a migration graph such that $m_{ij} = m > 0$ for all $i \neq j$. Consider an equilibrium P^{eq} with three degrees of freedom $P^{eq} = (p_1, p_2, p_{inter})$. Then, P^{eq} is solution to the 3-dimensional system of equations*

$$\begin{aligned} |V_2|h(p_{inter})(p_{inter} - p_1) + h(p_1)(1 - p_1) - \frac{\mu}{m}p_1 &= 0, \\ |V_1|h(p_{inter})(p_{inter} - p_2) + h(p_2)(1 - p_2) - \frac{\mu}{m}p_2 &= 0, \\ \frac{1}{2} \sum_{i=1}^2 (|V_i| - 1)h(p_{inter})(p_i - p_{inter}) + h(p_{inter})(1 - p_{inter}) - \frac{\mu}{m}p_{inter} &= 0. \end{aligned}$$

Proof Follows by construction of the equilibrium, namely, the partition of P^{eq} into the symmetry classes $\{P_{ij}^{eq} = p_k \text{ for } (i, j) \in V_k\}$ ($k = 1, 2$), and $\{P_{ij}^{eq} = p_{inter} \text{ for } (i, j) \in V_1 \times V_2\}$, and (27). \square

Assume now that h has a threshold. We want to show that there exists a stable, intransitive equilibrium in symmetric migration. Consider the friendship equilibrium $P^{eq} = (p_{ctr}, p_{fr}, p_{nofr})$ defined in Section 5, and c the threshold of the function h .

Proposition C.10 (Symmetry breaking II) *Let $M = ([N], (m_{ij})_{i \neq j})$ be a migration graph such that $m_{ij} = m > 0$ for all $i \neq j$. Consider a friendship equilibrium $P^{eq} = (p_1, p_2, p_{inter})$. Then, P^{eq} is solution to the 3-dimensional system of equations*

$$\begin{aligned} \frac{(N-3)}{2} h(p_{ctr})(p_{nofr} - p_{ctr}) + \frac{h(p_{ctr})}{2} (2 - 3p_{ctr} + p_{fr}) - \frac{\mu}{m} p_{ctr} &= 0, \\ (N-3) h(p_{nofr})(p_{nofr} - p_{fr}) + h(p_{ctr})(p_{ctr} - p_{fr}) + h(p_{fr})(1 - p_{fr}) - \frac{\mu}{m} p_{fr} &= 0, \\ h(p_{ctr})(p_{ctr} - p_{nofr}) + h(p_{nofr})(1 - p_{fr} + 2p_{fr}) - \frac{\mu}{m} p_{nofr} &= 0. \end{aligned}$$

Proof Same argument as in the proof of Proposition C.9. □

Remark C.11 *We remark that the two previous equilibria cease to exist for large N . In fact, consider the asymmetric equilibrium of Proposition C.9. We deduce from equation 1 and 2 that for large N , we need to have $h(p_{inter})(p_{inter} - p_k) \propto N^{-1}$, for $k = 1, 2$. Therefore, the two population groups V_1 and V_2 either become reproductively isolated from each other ($h(p_{inter}) \rightarrow 0$), or the equilibrium becomes symmetric ($p_{inter} - p_k \rightarrow 0$). The same argument allows us to deduce that there can only be a finite number of asymmetric equilibria for the equilibrium in Proposition C.10.*

D Additional simulations

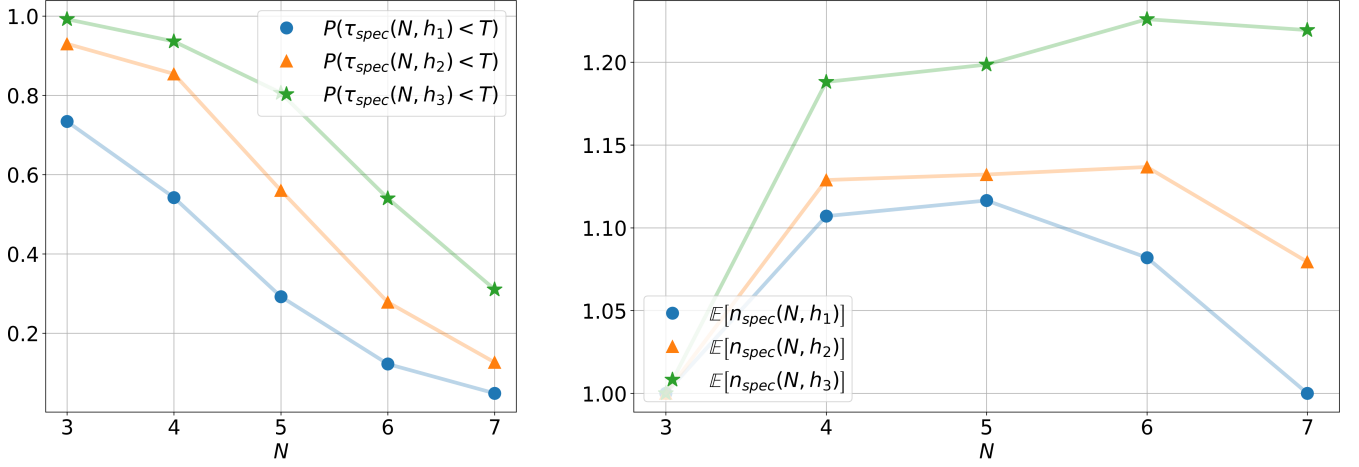


Figure 12: Decrease of speciation probability for different feedback regimes, and associated number of detaching populations. We considered dynamically changing migration rates updated according to exponential clocks and resampled *iid* according to a rescaled Beta distribution. We plotted an estimation of the probability of speciation before a given time (here, $T = 200$) for different feedback functions, see Fig. 10. Here, $h_1(x) = x^{2.5}$, $h_2(x) = x^{2.75}$, $h_3(x) = x^3$. Further, we chose $\mu = 0.1$, $m = \mathbb{E}[X] = 0.8375$, $\theta = 1$.

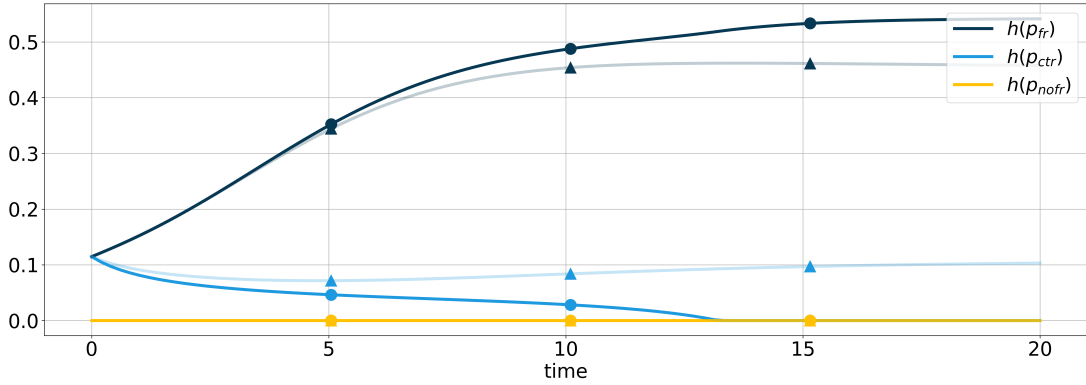


Figure 13: Collapse of intransitive friendship equilibria for large N (see Fig. 4a). The solid lines correspond to the three different genetic proximities in our system, namely the proximity between two populations at the outer points of the same triangle (p_{fr}), between the center population and a triangle population (p_{ctr}), and between two different-triangle populations (p_{nofr}). We used a step-feedback function similar to h_2 in Fig. 8. The migration structure is given by the friendship graph (see Fig. 4a) with $m = 0.5$, $\mu = 0.2125$. The different lines of a given color correspond to simulations for different values of N : $N = 11$ (triangle) and $N = 13$ (circle). For $N = 11$, the friendship graph is stable. For $N = 13$, a speciation event occurs.